AD-A150 032 SYSTEM IDENTIFICATION ANALYSIS OF INERTIA AND DRAG COEFFICIENTS FOR OFFSH..(U) HYDROMECHANICS INC PLAINVIEW NY P KAPLAN NOV 84 NCEL-CR-85-007 1/1

UNCLASSIFIED N62474-83-C-6728 F/G 8/3 NL

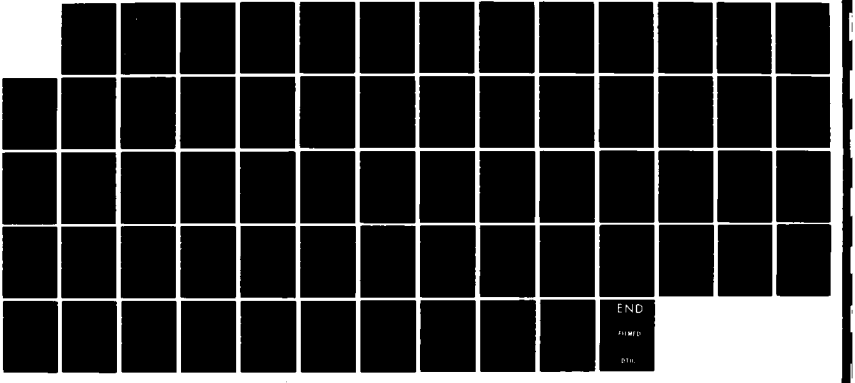

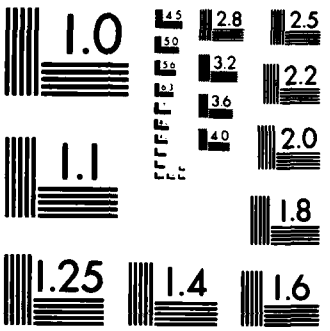

MICROCOPY RESOLUTION TEST CHART
NATIONAL BUREAU OF STANDARDS-1963-A

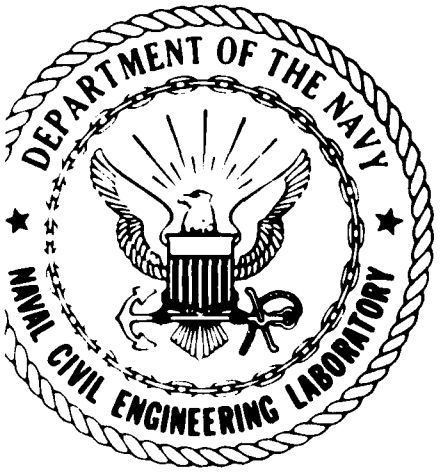

CR 85.007

NAVAL CIVIL ENGINEERING LABORATORY
Port Hueneme, California

Sponsored by
NAVAL FACILITIES ENGINEERING COMMAND

SYSTEM IDENTIFICATION ANALYSIS OF INERTIA AND DRAG COEFFICIENTS FOR OFFSHORE STRUCTURE FORCES DUE TO COMBINED OCEAN WAVES AND CURRENTS

November 1984

An investigation conducted by
Hydromechanics, Inc.
P.O. Box H
Plainview, New York 11803

N62474 83 C-6728

METRIC CONVERSION FACTORS

Approximate Conversions to Metric Measures

Symbol	When You Know	Multiply by	To Find	Symbol
		LENGTH		
in	inches	*2.5	centimeters	cm
ft	feet	30	centimeters	cm
yd	yards	0.9	meters	m
mi	miles	*1.6	kilometers	km
		AREA		
in^2	square inches	6.5	square centimeters	cm^2
ft^2	square feet	0.09	square meters	m^2
yd^2	square yards	0.8	square meters	m^2
mi^2	square miles	2.6	square kilometers	km^2
	acres	0.4	hectares	ha
		MASS (weight)		
oz	ounces	28	grams	g
lb	pounds	0.45	kilograms	kg
	short tons (2,000 lb)	0.9	tonnes	t
		VOLUME		
tsp	teaspoons	5	milliliters	ml
Tbsp	tablespoons	15	milliliters	ml
fl oz	fluid ounces	30	milliliters	ml
c	cups	0.24	liters	l
pt	pints	0.47	liters	l
qt	quarts	0.95	liters	l
gal	gallons	3.8	liters	l
ft^3	cubic feet	0.03	cubic meters	m^3
yd^3	cubic yards	0.76	cubic meters	m^3
		TEMPERATURE (exact)		
°F	Fahrenheit temperature	5/9 (after subtracting 32)	Celsius temperature	°C

*1 in = 2.54 (exactly). For other exact conversions and more detailed tables, see NBS Misc. Publ. 286, Units of Weights and Measures, Price $2.25, SD Catalog No. C13.10:286

Approximate Conversions from Metric Measures

Symbol	When You Know	Multiply by	To Find	Symbol
		LENGTH		
mm	millimeters	0.04	inches	in
cm	centimeters	0.4	inches	in
m	meters	3.3	feet	ft
m	meters	1.1	yards	yd
km	kilometers	0.6	miles	mi
		AREA		
cm^2	square centimeters	0.16	square inches	in^2
m^2	square meters	1.2	square yards	yd^2
km^2	square kilometers	0.4	square miles	mi^2
ha	hectares (10,000 m^2)	2.5	acres	
		MASS (weight)		
g	grams	0.035	ounces	oz
kg	kilograms	2.2	pounds	lb
t	tonnes (1,000 kg)	1.1	short tons	
		VOLUME		
ml	milliliters	0.03	fluid ounces	fl oz
l	liters	2.1	pints	pt
l	liters	1.06	quarts	qt
l	liters	0.26	gallons	gal
m^3	cubic meters	35	cubic feet	ft^3
m^3	cubic meters	1.3	cubic yards	yd^3
		TEMPERATURE (exact)		
°C	Celsius temperature	9/5 (then add 32)	Fahrenheit temperature	°F

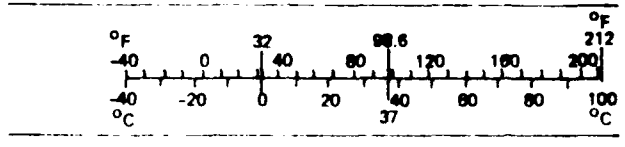

Unclassified

SECURITY CLASSIFICATION OF THIS PAGE (When Data Entered)

REPORT DOCUMENTATION PAGE		READ INSTRUCTIONS BEFORE COMPLETING FORM
1. REPORT NUMBER CR 85.007	2. GOVT ACCESSION NO. A150 032	3. RECIPIENT'S CATALOG NUMBER
4. TITLE (and Subtitle) System Identification Analysis of Inertia and Drag Coefficients for Offshore Structure Forces Due to Combined Ocean Waves and Currents		5. TYPE OF REPORT & PERIOD COVERED Final Sept. 1983-June 1984 6. PERFORMING ORG. REPORT NUMBER
7. AUTHOR(s) Paul Kaplan		8. CONTRACT OR GRANT NUMBER(s) N62474-83-C-6728
9. PERFORMING ORGANIZATION NAME AND ADDRESS Hydromechancis, Inc. P.O. Box H Plainview, New York 11803		10. PROGRAM ELEMENT, PROJECT, TASK AREA & WORK UNIT NUMBERS PE 62760N YF 60.534.091.01.A352
11. CONTROLLING OFFICE NAME AND ADDRESS Naval Civil Engineering Laboratory Port Hueneme, CA 93043		12. REPORT DATE November 1984 13. NUMBER OF PAGES 58
14. MONITORING AGENCY NAME & ADDRESS(if different from Controlling Office) Naval Facilities Engineering Command 200 Stovall Street Alexandria, VA 22332		15. SECURITY CLASS (of this report) Unclassified 15a. DECLASSIFICATION DOWNGRADING SCHEDULE

16. DISTRIBUTION STATEMENT (of this Report)

Approved for public release; distribution unlimited

17. DISTRIBUTION STATEMENT (of the abstract entered in Block 20, if different from Report)

18. SUPPLEMENTARY NOTES

19. KEY WORDS (Continue on reverse side if necessary and identify by block number)

Morison equation; waves; currents; wave forces; offshore structure; drag coefficient; inertia coefficient.

20. ABSTRACT (Continue on reverse side if necessary and identify by block number)

An analysis is made of the use of an extended Morison equation force model for determining the drag and inertia coefficients for an offshore structure subjected to a combined wave and current flow field. The method of analysis used is that of system identification, with this analysis applied to at-sea data obtained from the OTS investigation in the Gulf of Mexico.

DD FORM 1 JAN 73 1473 EDITION OF 1 NOV 65 IS OBSOLETE

Unclassified

SECURITY CLASSIFICATION OF THIS PAGE (When Data Entered)

The results support the use of the extended Morison model, but the force coefficient values do not indicate any definitive trend in terms of the current velocity parameter. The force coefficients found here are only useful as an additional contribution to a data base for establishing design ranges of such coefficients.

EXECUTIVE SUMMARY

An extended form of the Morison equation force model is considered for the case of an offshore structure vertical leg element in a combined wave and current flow field. The measurement data used in the analysis is that from the OTS/ investigation in the Gulf of Mexico, with the data in the form of 27-30 second wave segments containing velocity and force component measurements in two perpendicular directions in the horizontal plane. The analysis method used was the system identification technique that has been previously applied with success to similar type data when using the conventional Morison force model, with the objective being the determination of the drag and inertia force coefficient values together with the variation of these coefficients with different characteristic flow parameters.

A combined mathematical-computational analysis showed that the extended Morison model, when subjected to the procedures of the system identification method used, resulted in essentially the same type equations as for the conventional Morison model. Thus no separate determination of the current value, or the possible dependence of the force coefficients on any parameter involving the current, could be found from this analysis. The only possible dependence of the force coefficients on the current would be parametric, and would only be determined from analysis of the determined force coefficient values and their variation with characteristic dimensionless parameters.

The analysis of the force coefficient results shows the dependence of these coefficient values on such quantities as Reynolds number (Re), Keulegan-Carpenter number (KC), the ratio of current to wave velocity, etc. in both graphical and tabular form. There is no definitive dependence of the force coefficients on any current parameter, although there is some small indication of a reduction of C_D as the relative current-wave velocity ratio increases. The major utility of the present results is 222 sets of coefficients, applying to both smooth (painted) and slightly rough (unpainted) elements of an offshore structure, that represent part of a data base for establishing design ranges of such force coefficients for use in offshore structure design.

TABLE OF CONTENTS

	Page
INTRODUCTION	1
EXPERIMENTAL DATA	3
GENERAL DESCRIPTION OF ANALYSIS METHOD	7
MATHEMATICAL PROCEDURES FOR SEQUENTIAL ESTIMATION TECHNIQUE	9
DETERMINATION OF FORCE COEFFICIENTS IN MORISON EQUATION MODEL	13
Application to Combined Wave and Current	21
DIMENSIONAL ANALYSIS OF FORCE COEFFICIENTS	25
RESULTS OBTAINED AND DISCUSSION	30
CONCLUDING REMARKS	56
REFERENCES	57

INTRODUCTION

The usual mathematical model employed to represent the forces due to waves acting on a stationary offshore structure employs the Morison equation representation [1]. This particular method involves consideration of the force to be due to two different contributions, viz. an inertial force and a drag force. The inertial force involves an added mass (inertia) coefficient C_M which is associated with the fluid acceleration term, while the drag force employs a drag coefficient C_D which is combined with a velocity square term in that drag component. These coefficients have been determined from various laboratory and full scale investigations to depend upon certain fundamental parameters such as the Reynolds number (Re) and the Keulegan-Carpenter number (KC). A general discussion of the functional dependence of these coefficients, together with their use in representing forces on offshore structures, is given in a number of publication sources, e.g. [2] and [3].

Since this representation of wave forces has demonstrated some basic utility in practical applications for the offshore industry, in spite of certain fundamental objections from hydrodynamicists due to neglect of various fluid dynamic mechanisms, it has generally been adopted as the basic procedure in offshore engineering design studies. This same model has been used (in an extended form) for the case of moving elements such as risers, when considering structural vibrations together with wave-induced loads, etc. Some doubt has been raised concerning the utility of the Morison model when applied to moving bodies [4], although no definitive conclusion has been reached due to limited data available for detailed study and analysis.

Another important fluid motion condition where this same basic method of analysis is used is the case of combined wave and current velocities, where the current is a steady velocity flow. In most cases involving field measurements there is no separation between the current and the wave velocities since they occur together, and the associated data analysis does not allow for any distinction of the different contributing effects of these two different flows. As a result questions then arise as to the validity of the basis Morison equation model, as well as the magnitude and functional dependence of these force coefficients in such a model in terms of the various parameters associated with such a flow field. Some indication of the effect of a current on the force coefficients for an offshore structure has been given by Sarpkaya [5], where this effect has been considered as a partial explanation of scatter in results of conventional data analysis techniques applied to the Ocean Test Structure in the Gulf of Mexico (see [6]).

In order to study this problem it is necessary to have available an adequate set of data obtained in an ocean environment, as well as a suitable technique for analysis that could provide the desired force coefficients. A description of the basic experimental data set, the method of analysis applied, and the results of the data analysis procedure are provided in the following sections of this report.

EXPERIMENTAL DATA

The experimental data set selected for analysis in this investigation was that from the Ocean Test Structure (OTS) project in the Gulf of Mexico. A description of the OTS and the initial basic study associated with that particular offshore platform is given in [7].

The data measurements obtained on the OTS which are of interest in the present study are the velocities and forces measured on a segment of a vertical member placed below the MWL, in which the force sensor system is included. A description of the coordinate system and sign convention used is shown in Figure 1, where the angle α represents the direction in which the waves are propagating. The wave force sensors are located at the four vertical corner legs at a depth of 15 ft. below the MWL. The forces measured are the x- and y-components of the horizontal force. The diameter of the sensor is d=16 in. (nominal diameter) and the length L=2d=32 in. The NW sensor is painted (to inhibit marine growth biofouling) and the SW sensor is unpainted. Most of the data analyzed here was for the NW sensor, while some information was also presented for the SW sensor which would reflect some influence of marine growth in the results. The force coefficients are calculated with respect to the nominal diameter, with no consideration of any increased effective diameter that would be caused by marine growth. Current velocity meters measure the x- and y- components of the horizontal velocity at points close to the force sensors.

The data was obtained during the winter period 1976-1977, from which particular waves were selected for analysis. All of the necessary measurements obtained in the entire test program are provided on a digitized magnetic tape that was originally supplied by Exxon Production Research Co. (EPR). The various force measurements were initially filtered, using an analog 4-pole Butterworth filter having a cutoff frequency of 3 Hz., and then recorded on magnetic tape recorders. It is this data that was processed and digitized, with the final data for all recorded channels provided on the digital magnetic tape at a sample rate of 10 samples/sec. Thus the digital information would provide data having validity (in the frequency domain) up to 5 Hz., without considering any effect of the filter that could affect responses at frequencies greater than 2 Hz. However such short waves would have no effect on the present study, and hence the digital records are considered as proper representations of all of the measured variables.

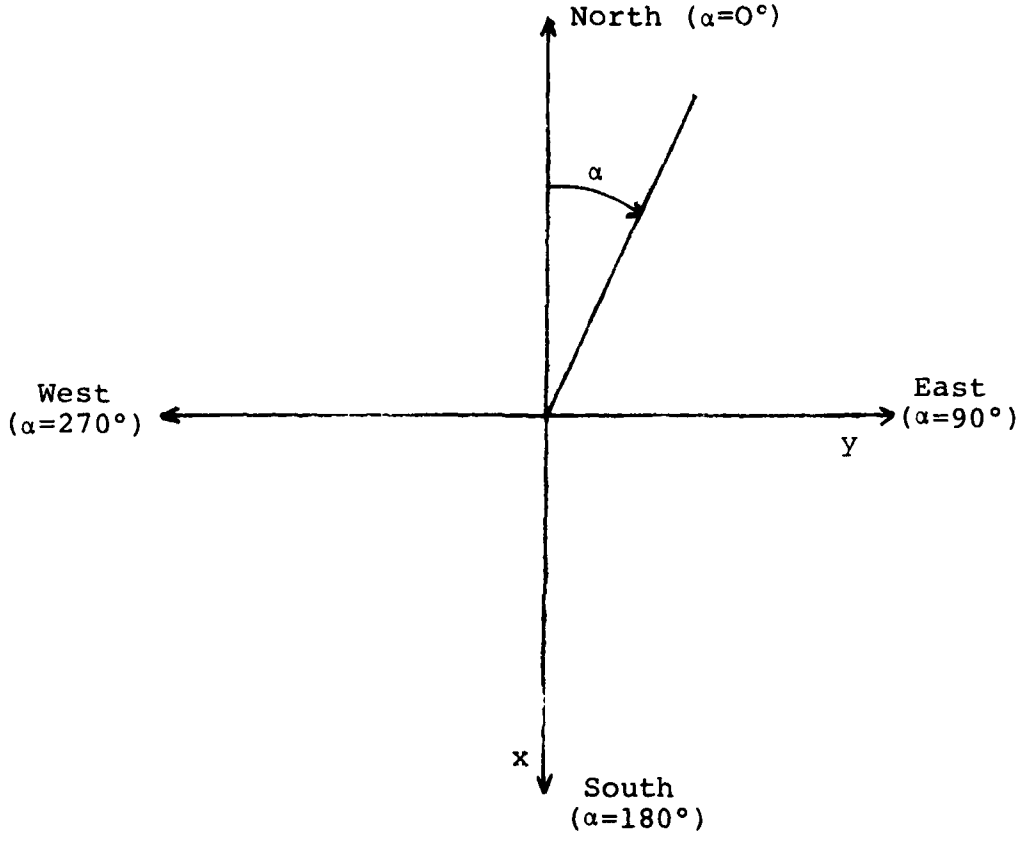

Fig. 1 Orientation of OTS coordinate system

The OTS project selected a number of large wave segments of about 30 sec. length (each) which were to be analyzed for the 1976-1977 winter period. One particular set, denoted as the Conductor Group Waves (C waves), was comprised of 55 separate wave segments (30 sec. segments). While analyses were made for all of these C waves as part of the OTS investigation, it was found that only the first 38 waves (C-1 to C-38) that occurred in days 10 and 54 (of the year 1977) were valid measurements for the NW (painted) sensor. The remaining waves in the C-series, as well as about all of another wave group (s-waves), gave invalid measurements in that winter recording season due to zero drifts in the force measurements as well as similar type problems in the current measurements for the NW sensor. However, all of the SW force sensor data was valid for the 55 C waves.

Another data set from the OTS investigation contained a number of separate one hour long continuous records obtained during the 1976-1977 winter season measurements. Those records contained similar force and velocity measurements as above, together with other related measurements in the overall OTS project. These records, in time history form, were used to determine various power spectral densities, with the method of analysis, description of the tape recording format, and illustrative plots of the results of spectral analysis given in [8].

Examination of the description of the measurement records in [8] shows that in only one of the records were there coincident measurements of wave forces and the local wave velocities at the same location; i.e. at the NW leg element at 15 ft. depth. In all of the other records the forces were measured at a particular leg location, while the velocity records were made at another leg location (SE, across the platform structure) which was at the same depth (15 ft.) as the force measurement. That particular type of measurement arrangement would not affect spectral analysis results, but would have an influence on the time domain analysis required to determine the Morison equation force coefficients. It is then necessary to apply an analytical procedure that corrects for such a separation distance between the force measurement location and the velocity measurement location by appropriate "transport" relations (e.g. see [9]). Experience in [9], as well as other studies involving wave property transport operations, showed that such operations did not have a noticeably large effect on any final derived results (differences of only 2-3%). Thus data from [8], which included the SW leg force sensor and velocity measurements at the SE leg, was also available for analysis purposes when applying this wave property transport operation.

The particular record that satisfied the requirement of coincident measurements was identified as corresponding to wave tape LS8A, with the measurements made on day 54 of 1977. Thus the coincident measurements at the NW leg in tape LS8A were then used to select 124 separate 27 sec. long wave segments for use in an analysis to determine the required force coefficients. These records from LS8A, together with the 38 C waves described previously, comprise a data set of 162 separate records for the painted NW sensor that are available for analysis purposes in the present study. In addition, in order to provide a larger set of conditions that would have larger currents as well as reflect some effect of limited marine growth, data was also obtained from wave tape SS9 of [8]. That particular data was obtained on day 63 (March 4) of 1977, with the force measurements on the SW leg. There were 60 separate 27 sec. long wave segments selected from tape SS9 for the SW sensor which were then also used for analysis as part of the present investigation.

GENERAL DESCRIPTION OF ANALYSIS METHOD

The particular method to be applied to determine the force coefficients is a procedure that has been used to determine the values of various parameters in a mathematical representation of the dynamics of an arbitrary system, and has been developed as a part of modern control theory. This procedure is known as "system identification," which in the present case is a means of determining the numerical values of the coefficients that enter into a set of mathematical equations which are assumed to represent the dynamics of that system. In addition the procedure can also determine the suitability of a particular mathematical form, as well as the sensitivity of particular outputs to certain coefficients. The values of the coefficients determined from such an analysis are considered to be the appropriate numerical values representing the system when they are found with the same basic values from a number of different time histories of the basic force, under the same conditions that characterize each time history, (e.g. Reynolds Number, Keulegan-Carpenter Number, etc.), which would then insure uniqueness of these values for those conditions.

What is done in this technique is to obtain the responses of the system from the force measurements, together with the elements that are assumed to create these forces such as the velocity field adjacent to the force measuring element on the structure. Using the Morison equation as the basic mathematical model the values for the unknown parameters are then sought so that the representation of the corce by the model gives a best fit to the data, where this best fit is defined by minimizing the mean square error between the computation of the force using these coefficients (and the recorded velocity time histories) and the actual force data record itself.

The mathematical procedure used involves the representation of the basic equation for the force in terms of the unknown coefficients, and the coefficients themselves are then the actual variables that are sought. In this procedure it is assumed that they are constants throughout the time in which the particular wave and velocity time histories are examined, i.e.,

$$\frac{dC_M}{dt} = \frac{dC_D}{dt} = 0 \qquad (1)$$

where Equation (1) is the applicable relation for the coefficients as additional state variables that are subject to the basic constraint equation. It is necessary to obtain measurements of other state variables associated with the force representation in this method of system identification, and the choice of what has to be measured is made in establishing the particular investigation (to be discussed in more detail in the following section).

There are a number of different procedures of system identification which can be applied according to whether transient dynamics or the case where random function time histories are involved, or the situation where there are measurement observation errors present. The techniques are quite different and a general description of procedures used for determining coefficients of different dynamic systems, under different operating conditions of interest to naval applications, is presented in [10]. In the present case the method applicable to random function excitation, including the presence of measurement noise, would be the most useful for determining the required coefficient values. The method inherently includes an on-line filtering procedure together with a sequential estimation technique which does not require repeating all calculations after earlier calculations are made, as in classical estimation schemes. Continuous measurements of the force system outputs are observed and operated on, together with the time histories of the measured velocities, leading to an evaluation of the desired parameters to be generated as functions of time that readily approach their final steady value. It is possible that a particular single (individual) wave time history would not be of sufficient time extent to allow the coefficients to reach their final values, so that the overall time history (used in this type of analysis) will be that for the 30 sec. time period selected for analysis on the magnetic tape records prepared in the OTS project (covering more than one individual wave) which is expected to form an adequate time period for determining the parameters appropriate to that condition.

The method will be applied to both of the two measured horizontal force components, using the measured velocity from the current meters adjacent to each particular force sensor in the vertical leg which is coated with antifouling paint. The output of the analysis of this data will provide the appropriate values of C_M and C_D that are considered appropriate to each particular record analyzed in this task. Values of Reynolds Number and other pertinent parameters influencing these coefficients will also be determined for each wave run, allowing the force coefficient values to be correlated with these parameters. The application of this system identification technique to evaluate the force coefficients for offfshore structures is a novel extension of advanced technology and computational procecures that have previously been successfully applied to vehicle dynamics and control systems. A description of the mathematical procedures for the sequential estimation technique applied in this study is given in the following section.

MATHEMATICAL PROCEDURES FOR SEQUENTIAL ESTIMATION TECHNIQUE

When considering the use of system identification for cases where the observed data is contaminated by noise or if the system is excited by a random input, the method that is used is based upon a sequential estimation procedure that is derived as illustrated below. The basic problem underlying this system identification technique is that of estimating the state variables and the parameters in a noisy nonlinear dynamical system, and this problem is treated in [11], which is an extension of the simpler problems where only observation errors occur [12]. Considering the scalar case (i.e. a single state variable), the system is represented by

$$\dot{x} = g(x,t) + k(x,t)\ v(t) \tag{2}$$

where $v(t)$ is the unknown disturbance input. The measurements or observations of the output are

$$y(t) = h(x,t) + (\text{measurement errors}) \tag{3}$$

No assumptions regarding the statistics of the unknown input functions or the measurements error is made. With measurements of the output $y(t)$, for $0<t<T$, it is required to estimate $x(T)$ on the basis of minimizing with respect to $\bar{x}(t)$ (a nominal trajectory) the functional

$$J = \int_0^T \left| e_1^2(t) + w(\bar{x},t)\ e_2^2(t) \right| dt, \tag{4}$$

where $w(\bar{x},t)$ is a positive weighting factor, and the errors e_1 and e_2 are defined by

$$e_1(t) = y(t) - h(\bar{x},t)$$

$$e_2(t) = \dot{\bar{x}} - g(x,t) \tag{6}$$

The least squares estimate of $x(T)$, denoted as $\hat{x}(T)$, is obtained from minimizing the integral of the (weighted) mean square errors, where the error $e_2(t)$ represents the difference between a nominal trajectory and the assumed form of its equation representation.

The minimization problem is then a problem in variational calculus, which leads to the associated Euler-Lagrange equations that contain an unknown Lagrange multiplier. The boundary conditions for this Lagrange multiplier are known at the ends of the interval, i.e. 0 and T, but there is no information about the

value of x(T), and hence the problem reduces to a two point boundary value problem (TPBVP) that yields the optimal estimate $\hat{x}(T)$. With the variable T now considered as a running time variable, the problem is treated as a family of problems with different final points, T, and the problem becomes one of sequential estimation, i.e the TPBVP must be continuously solved for all values of T (the running time variable).

The problem is solved by application of the concept of invariant imbedding []3], which is used to convert a TPBVP into an initial value problem that can be easily solved. The missing "initial condition" is represented in a general manner for different values of T, thereby establishing a family of problems. On the basis that neighboring processes (i.e. system responses) are related to each other, the missing condition is found by examining the relationships between such neighboring processes. The procedure leads to a partial differential equation that is solved by an expansion of the solution about the desired reference condition, which in the present case is the estimate $\hat{x}(T)$ (see [11]. The result of this invariant imbedding approach is a sequential estimator, which is such that previous data points do not have to be repeated whenever new observations are added, and hence the estimation operation can be carried out at a fast computational rate.

The estimator equations for the scalar case are

$$\frac{d\hat{x}}{dT} = g(\hat{x},T) + 2P(T)h_{\hat{x}}(\hat{x},T)\left[y(T)-h(\hat{x},T)\right] \tag{7}$$

$$\frac{dP}{dT} = 2P(T)g_{\hat{x}}(\hat{x},T) + 2P\frac{\partial}{\partial x}\left\{h_{\hat{x}}(\hat{x},T)\left[y(T)-h(\hat{x},T)\right]\right\}P + \frac{1}{2w(\hat{x},T)} \tag{8}$$

where

$$h_x = \frac{\partial h(\hat{x},T)}{\partial \hat{x}}, \qquad g_x = \frac{\partial g(\hat{x},T)}{\partial \hat{x}} \tag{9}$$

The above results are somewhat similar to, and represent a generalization of the results of linear Kalman filtering [14]. The weighting function P(T) is found from a Riccati-type equation, and the two equations are solved when given the initial conditions. The initial value $\hat{x}(0)$ represents the

best estimate of the system state at t = 0, which is based on available a priori information, and the initial value P(0) reflects the confidence in the initial value of $\hat{x}$ and the observed signal y(t).

The estimator equations for the vector case are derived in [11] and are given below as

$$\frac{d\hat{x}}{dT} = g(\hat{x},T) + 2P(T)H(\hat{x},T)Q\left\{Y(T)-h(\hat{x},T)\right\} \tag{10}$$

$$\frac{dP}{dT} = g_{\hat{x}}(\hat{x},T)P + Pg'_{\hat{x}}(\hat{x},T) + 2P\left[HQ\left\{Y(T)-h(\hat{x},T)\right\}\right]_{\hat{x}} P + \frac{1}{2}\, k(\hat{x},T)V^{-1}(\hat{x},T)k'(\hat{x},T) \tag{11}$$

where

$$H(x,T) = \frac{\partial h(x,T)}{\partial \hat{x}}' \tag{12}$$

(' symbol represents transpose of matrix), Q is a normalizing matrix used to weight the observation errors in the minimization procedure, the function $k(\hat{x},T)$ is a coefficient of the unknown input forcing function (as in Equation (2), but for the vector case), and the function $V(\hat{x},T)$ is defined by

$$V(\hat{x},T) = k'(\hat{x},T)W(\hat{x},T)k(\hat{x},T) \tag{13}$$

with W the weighting matrix for the errors in the basic equations due to the input disturbances. In the estimator equations the term $[HQ\{Y(T) - h(x,T)\}]_{\hat{x}}$ is an nxn matrix with i^{th} column given by

$$\frac{\partial}{\partial x_i}\left[HQ\left\{Y(T) - h(\hat{x},T)\right\}\right] \tag{14}$$

The basic equations of the system and its observations are similar to those of Equations (2) and (3) but generalized to the vector case. With x an n-vector, P(T) is an nxn matrix, so that the number of equations required to be solved are n^2+n which can become a large computational task. Some possible simplification could occur in some cases where the P-matrix has symmetry for the off-diagonal terms, depending on the form of the functions H, Q, etc., thereby leading to a reduction of the number of equations to be solved.

In the case where identification of parameters is considered, the constant (but unknown) parameters, denoted as a vector a (with m elements), satisfy the differential equation

$$\frac{da}{dt} = 0 \qquad (15)$$

and the m elements of a can be considered as additional elements in the state vector, i.e. they are adjoined to the state vector elements (ℓ elements) so that $n_{\hat{x}} = \ell + m$ is the total number of elements in the state variable $\hat{x}$, which also includes the estimates of the m unknown parameters in a. The equations given in Equation (15) are easily absorbed into the total system representation in establishing the g-matrix, and the remaining equations for P readily follow. The only problem resulting from the introduction of the additional elements is the increase in the total number of equations to be solved, which increases the computational complexities. The application of the mathematical procedure described here to the problem of determining the force coefficients of the Morison equation is discussed in a later section of this report.

DETERMINATION OF FORCE COEFFICIENTS IN MORISON EQUATION MODEL

The initial application of this method of system identification to determine the Morison equation force coefficients on an offshore structure (OTS) subjected to wave action was described in [15]. In that case the Morison equation was expressed for the vector wave force acting on the test section as

$$\frac{d\vec{F}}{dz} = C_M \frac{\pi \rho D^2}{4} \dot{\vec{u}} + C_D \frac{\rho D}{2} \vec{u}|u|$$

where $d\vec{F}$ = wave force acting on the axial segment dz of a cylinder

ρ = water density

$\vec{u}$ = fluid velocity

$\dot{\vec{u}}$ = fluid acceleration

After substituting g = 32.2 ft./sec.^{2}, D = 16 in., ρ = 1.99 slug/ft.^{3} and Δz - 32 in. into the last equation, it can be shown that Equation (16) is expressed as

$$F_j = 7.41 C_M \dot{u}_j + 3.54 C_D u u_j \qquad (17)$$

for the force component (F_x and F_y) in terms of the velocity and acceleration components, where j = x for the south component or y for the east component. The resultant fluid speed u is defined as

$$u = \sqrt{u_x^2 + u_y^2} \qquad (18)$$

and the problem is to find the coefficients C_M and C_D.

In order to apply this method of system identification to the present case of the Morison equation, it is necessary to have a dynamic system that is represented by a differential equation. The wave force is not part of a "dynamic "system" of this nature, but is only an observable measurement. The only dynamic system considered proper for this problem was that for the velocity field, since the velocity field was measured and the wave force components are represented in terms of the fluid velocities (and accelerations), with the force coefficients included as part of the Morison equation force model.

The mathematical model for the velocity field was then represented in the general form

$$\ddot{u} = f(t) \tag{19}$$

where f(t) is an arbitrary random function of time. A second order equation was selected since there are 2 unknown coefficients that have to be determined, and this particular model also allows for the presence of a current (i.e. a constant value) as well as an irregularly varying portion in the velocity. It is this model that was used in the basic analysis of [15], with the equations structured as shown in the following.

Defining the six state variables

$$x_1 = \dot{u}_x \ , \ x_2 = \dot{u}_y \ , \ x_3 = u_x \ , \ x_4 = u_y \ , \ x_5 = 7.41 \ C_M \ ,$$

$$x_6 = 3.54 \ C_D \tag{20}$$

the system equations, following the basic model and analysis given in the preceding section, are

$$\begin{aligned} \dot{x}_1 &= k_1 v_1 \\ \dot{x}_2 &= k_2 v_2 \\ \dot{x}_3 &= x_1 \\ \dot{x}_4 &= x_2 \\ \dot{x}_5 &= 0 \\ \dot{x}_6 &= 0 \end{aligned} \tag{21}$$

where v_1 and v_2 are unknown inputs. The measurements are made of the time histories of velocities and forces, represented by

$$\begin{aligned} y_1 &= \text{observed velocity in x-direction} \\ y_2 &= \text{observed velocity in y-direction} \\ y_3 &= \text{observed force in x-direction} \\ y_4 &= \text{observed force in y-direction} \end{aligned} \tag{22}$$

The assumed mathematical model for these measured quantities is given by the h-vector, with component elements defined by

$$h_1 = x_3$$

$$h_2 = x_4$$

$$h_3 = x_5x_1+x_6x_3\sqrt{x_3^2+x_4^2} \tag{23}$$

$$h_4 = x_5x_2+x_6x_4\sqrt{x_3^2+x_4^2}$$

where these mathematical models correspond to the particular measured quantities (y-values) with the same subscript.

The digital computer program is established for solution of these coupled first order differential equations, corresponding to the estimator equations defined in Eqs. (10) - (14). They are nonlinear and time-varying, in general, and the technique for solution is based upon use of a Runge-Kutta fourth order integration scheme. The integration time step is given as input (in the program) and can be less than the measurement interval (0.1 sec.). The value of time step to be used in integration would depend upon requirements of stability, total time of solution, etc. All of the computer operations for a general equation system are carried out in matrix form, as indicated by the representation of the equations given in a preceding section, and various subroutines to make use of matrix manipulations are employed which are standard procedures associated with digital computer operations. The results of application of these equations for determination of the force coefficients in Morison's equation are discussed below, together with additional information on numerical values and procedures in the computations.

The velocity and force have different numerical magnitudes. It is important to choose appropriate weighting matrices of Q and W (or V) in order to get stable results. The following weighting factors were adopted for the calculation:

$$Q = \begin{bmatrix} 1 & & 0 \\ & 1 & \\ & & .0005 \\ 0 & & & .0005 \end{bmatrix} \tag{24}$$

$$\frac{1}{2} KV^{-1}K' = \begin{bmatrix} 100 & & & & & \\ & 100 & & & & \\ & & 0 & & & \\ & & & 0 & & \\ & & & & 0 & \end{bmatrix} \qquad (25)$$

The matrix Q represents the inverse of the observation errors, by analogy to the form of Kalman filtering (see [14] and [16]), and it is assumed that the observation errors are generally small for the fluid velocities. The Morison equation model is a "fit" to the actual force, so that it is expected that there would generally be a more significant error in that type of model relative to the actual force, which in the present context would thereby be a larger "measurement error". Thus the basis for the indicated values of the diagonal elements in the Q-matrix in Equation (24).

The matrix representing $\frac{1}{2} KV^{-1}K'$ in Equation (25) corresponds to the random forcing function in the differential equation for the state variables. Since there is a random forcing function for the state variables x_1 and x_2, the equations for x_3 and x_4 are exact according to the basic model, and the variables x_5 and x_6 are considered to be constants in the present analysis, then the values given in the diagonal matrix elements in Equation (25) represent that situation. The particular values used in these matrices shown in Equation (24) and (25) are also based upon values indicated in the work of [10] and [11], as well as upon the results of stability and convergence of the equations when carrying out numerical experiments (related to the work reported in [15]).

The initial velocity value estimates can be assumed to be equal to the measured velocities. The matrix P and the final value of the force coefficients are fed back as initial conditions after each 30 sec. record period, with each 30 sec. record period being used as many times as necessary to arrive at final converged values of the force coefficients together with good "tracking" of the estimated values of velocities, force components, etc. as compared to the actual measured values. Each use of a 30 sec. record length during the analysis of that particular wave record and associated measurements is referred to as an "iteration" in the analysis procedure used in the work of [15]. Convergence tests of the estimated force coefficients illustrate the effective asymptotic convergence to the final coefficient values after a number of iterations, as shown in Figure 2. The final values at the final iteration run shows that the force coefficient values are just about constant throughout the 30 sec. record (see following discussion).

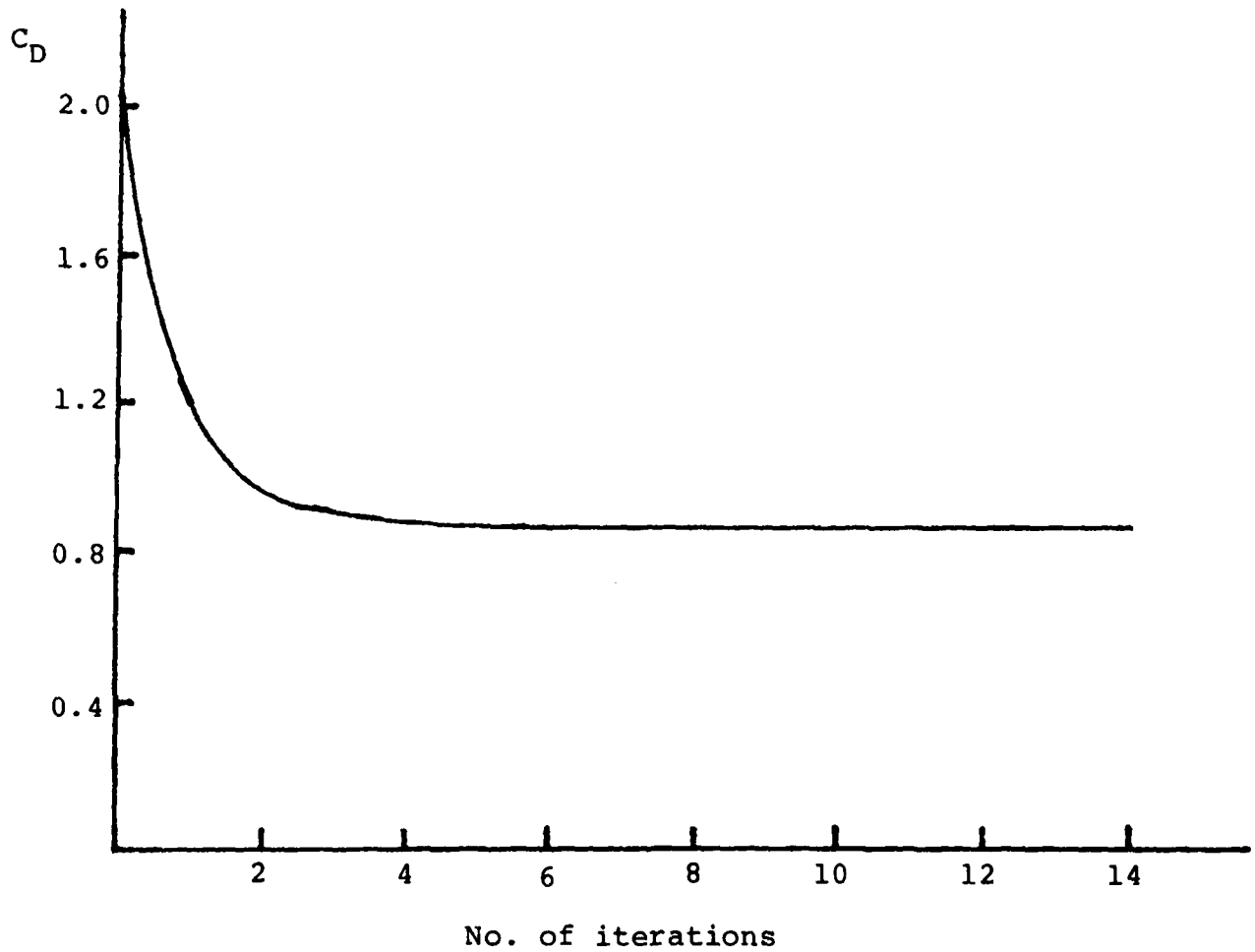

Fig. 2 Variation of C_D with no. of iterations, C-45 record.

An example of the correspondence between the measured data and the estimated results obtained by the system identification procedure, as reported in [15], is shown in Figures 3 and 4, where the instantaneous C_M and C_D values are used to calculate the estimated forces. The values of C_M and C_D in that same 30 sec. period are presented in Figure 5 and demonstrate that these numbers are fairly constant, which is the nature of the results indicated in other applications of system identification (see [10] and [11]). The results obtained here indicate that the present system identification technique, when applied to determine the Morison equation force coefficients, can provide a valid result.

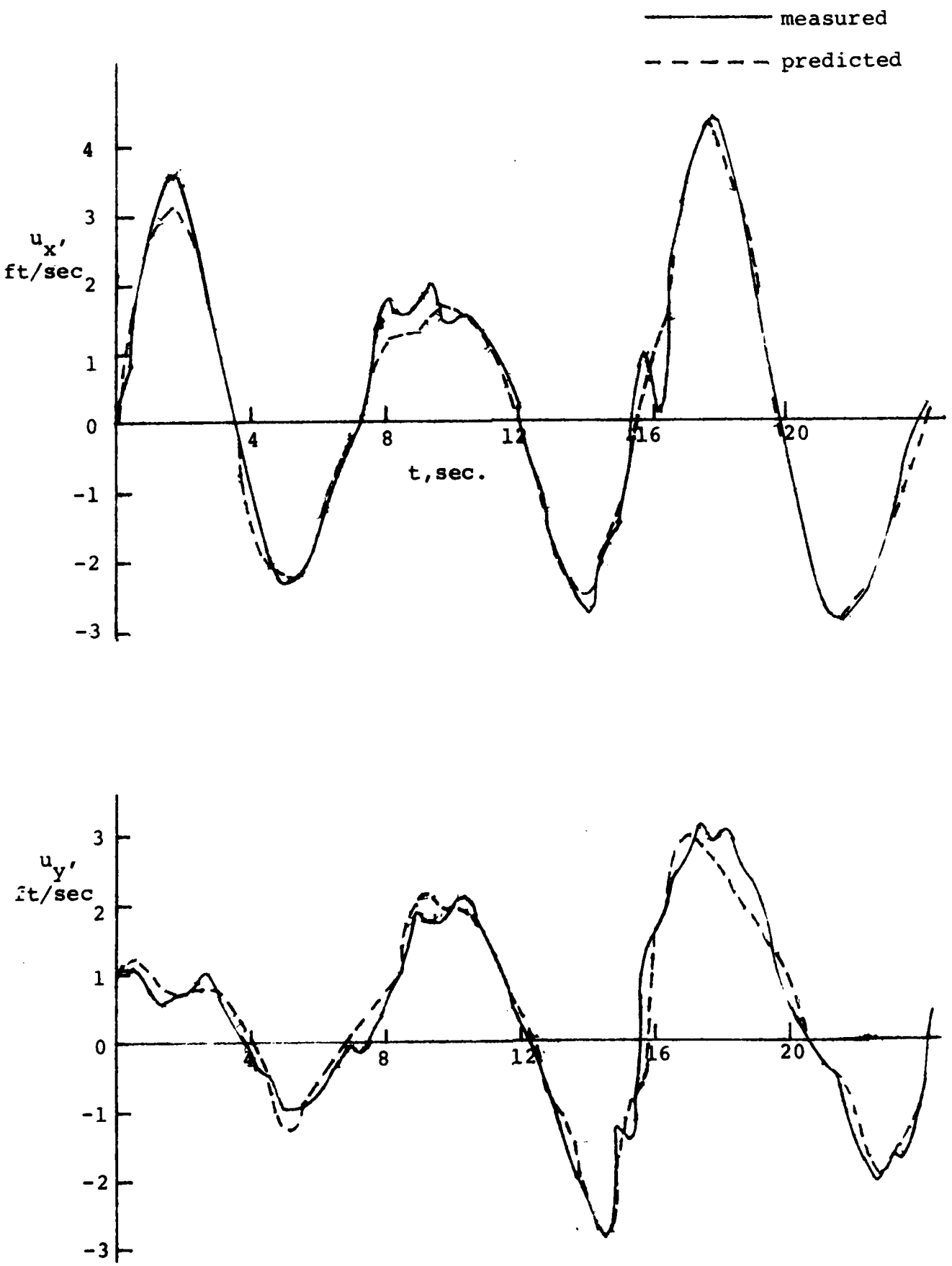

Fig. 3 Comparison of measured and predicted velocities, C-25 wave record.

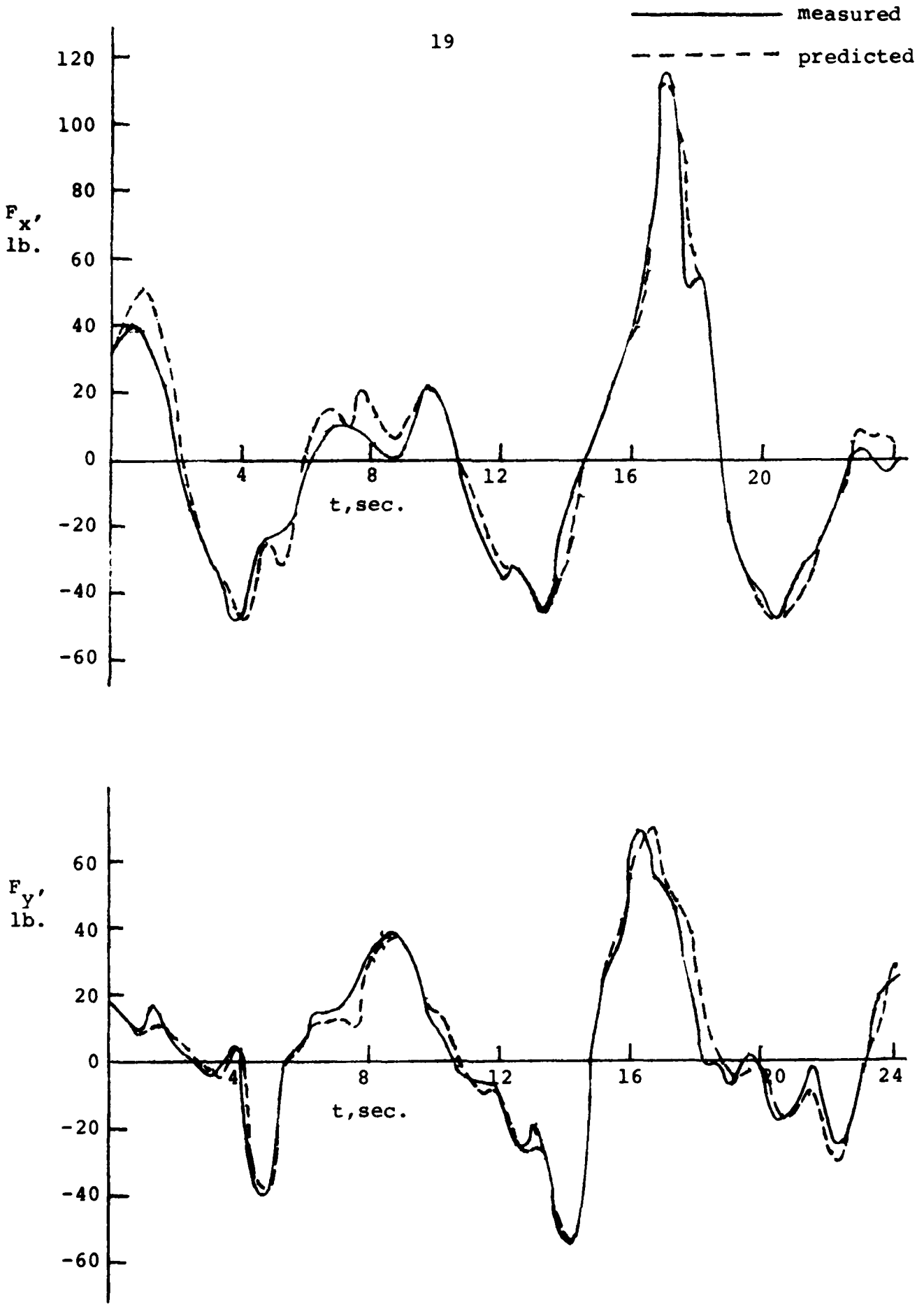

Fig. 4 Comparison of measured and predicted forces, C-25 wave record.

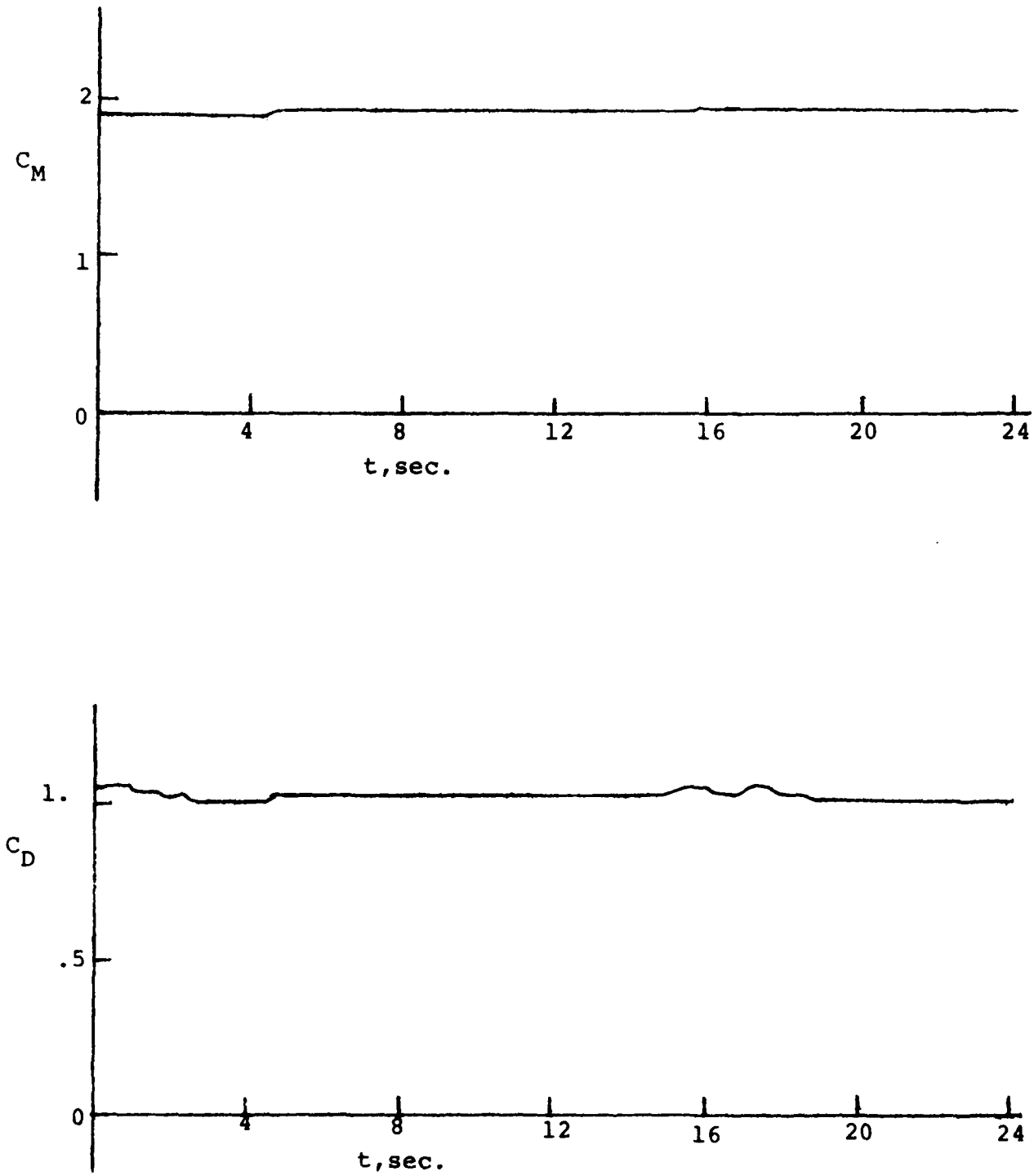

Fig. 5 Time histories of C_M and C_D, final iteration, C-25 wave record.

The method employed here, and illustrated by the results in Figures 2-5, exhibits certain features that can be contrasted with results found by other methods of analysis (e.g. [6]). Observation of the time histories of the velocities, forces, etc. as estimated by the identification method, when compared to the measured values, indicate how well the estimated variables "track" the actual measurements. This type of output and comparison in on-line form is directly obtained in the present analysis, which provides a measure or check on the utility of the method. The basic method inherently contains an on-line filtering action which provides an optimum filtering of the measured velocities and forces so that extraneous effects are eliminated. Thus there is no need to apply separate (and subjectively selected) filtering to the measured data before applying any analysis procedures. Another feature of this method is that the optimum accelerations are also provided by the appropriate state variable estimates, which eliminates the need for direct differentiation, introduction of large noisy signals, filtering procedures, etc. that would ordinarily be required by conventional procedures. The present analysis technique is applied to the entire 30 sec. wave record (and associated measurements) rather than to a limited wave segment, and the values of C_M and C_D found for each wave record are appropriate to the entire time histories given in each record.

Application to Combined Wave and Current

The procedure described above was developed and applied to cases of wave velocity disturbances, with the illustrations given in Figures 2 - 5 as representative of the results obtained by this method (see [15]). For the case where a steady current is present together with the wave flow field, another mathematical model that represents a generalization of the basic Morison formula is generally used in the offshore industry. In that case the velocity is defined in terms of the separate current and wave velocity summed, i.e.

$$u_x \rightarrow u_{x_o} + u'_x$$
$$u_y \rightarrow u_{y_o} + u'_y \qquad (26)$$

where the o-subscript represents the current componet and the primed (') terms represent the time-varying wave velocity component. Since the currents are steady there is no effect on the acceleration, with the acceleration terms only due to the time-varying flow components.

With the current values as known quantities, the state variables are defined in a similar manner as the previous case; i.e.

$$x_1 = \dot{u}'_x \ , \ x_2 = \dot{u}'_y \ , \ x_3 = u'_x \ , \ x_4 = u'_y \ ,$$
$$x_5 = 7.41 \ C_M \ , \ x_6 = 3.54 \ C_D \tag{27}$$

The system equations are also essentially the same as in Eq. (21), but using the primed variables. The assumed mathematical representation of the measurements are given by

$$h_1 = x_3 \ , \ h_2 = x_4$$
$$h_3 = x_5 x_1 + x_6 (u_{x_o} + x_3) \sqrt{(u_{x_o} + x_3)^2 + (u_{y_o} + x_4)^2}$$
$$h_4 = x_5 x_2 + x_6 (u_{y_o} + x_4) \sqrt{(u_{x_o} + x_3)^2 + (u_{y_o} + x_4)^2} \tag{28}$$

with each of these models corresponding to the measured variables $y_1 - y_4$.

The g-function (defined in Eq. (2) and its generalization to the vector case) for this case is the same as the previous case of only wave velocities, and the other necessary matrix quantities used in the identification-estimation procedure were also determined. The H-matrix, defined in Eq. (12), is a 6x4 matrix here as in the previous case, with similar type elements. Since the current values are known, the time-varying part of the measured velocity is determined by simple subtraction so that it can be compared to the state variable estimate, etc., as required in the present identification procedure. However, a detailed examination of all of the equations, the matrix element terms, etc. shows that the only change in this system is the replacement of the velocity definition given by Eq. (26) for the basic velocity terms. Thus the quantity $(u_{x_o} + x_3)$ appears in every matrix element term here instead of x_3 in the original case, with similar replacements for the x_4 variable, etc. If the original variables are redefined to include the current values then the present set of equations reduces exactly to that for the case treated in [15]. As a result there will be no difference in any of the force coefficient values found by the analysis, whether a current is considered or not, for any particular 27 - 30 record wave segment that is analyzed, i.e. the same force coefficients, degree of force time history matching, etc. will be found.

In order to establish a mathematical model that could possibly reflect the influence of currents in a more direct manner, the equations were reformulated in order to consider the current values as unknown constants that were to be found. The state variables are then defined as

$$x_1 = \dot{u}_x \ , \ x_2 = \dot{u}_y \ , \ x_3 = u_x \ , \ x_4 = u_y \ , \ x_5 = 7.41 \ C_M \ ,$$

$$x_6 = 3.54 \ C_D \ , \ x_7 = u_{x_o} \ , \ x_8 = u_{y_o} \qquad (29)$$

and the system equations are

$$\dot{x}_1 = k_1 v_1 \ , \ \dot{x}_2 = k_2 v_2 \ , \ \dot{x}_3 = x_1 \ , \ \dot{x}_4 = x_2 \ ,$$

$$\dot{x}_5 = 0 \ , \ \dot{x}_6 = 0 \ , \ \dot{x}_7 = 0 \ , \ \dot{x}_8 = 0 \qquad (30)$$

The matrices in the identification - estimation equations extend up to 8x8 in this case, as compared to 6x6 in the original system. All of the necessary operations to establish these equations were carried out and the computer program also established for this case.

Some wave segments were selected for analysis and the original method applied in order to obtain values of the Morison equation force coefficients by means of the basic identification procedure described previously. These cases provided satisfactory matching of the measured forces and velocity time histories when applied to cases for the painted NW sensor, which indicated that the procedure was functioning properly. Attempts were then made to apply the mathematical model based upon the relations in Eqs. (29) and (30) to the same wave records, in order to determine the unknown force coefficients as well as the values of the current components in that mathematical model. A number of different attempts were made and it was found that the solutions did not behave properly, causing numerical overflow (i.e. "blowing up") as well as not tracking the measured data. This behavior was exhibited in the early time period of the solution, thereby indicating the existence of a significant problem.

A number of different computer experiments were attempted, all leading to the same basic result of numerical overflow. A detailed examination of the program did not reveal any errors, leading to an examination of the fundamental equations that were structured for this case, i.e. as shown in Eqs. (29) and (30). It can be seen from an examination of all of the associated operations in establishing the equations that the combination $(x_3 + x_7)$ always appears together and similarly the combination $(x_4 + x_8)$ also appears together, with each term essentially replacing the quantities x_3 and x_4, respectively, from the

original equations. It can also be seen that the equation $\dot{x}_3 = x_1$ can be replaced by $(\dot{x}_3 + \dot{x}_7) = x_1$, with a similar relation involving $(x_4 + x_8)$.

What this means is that the equation system described by Eqs. (29) and (30) can be easily changed to be equivalent to that in Eqs. (20) and (21) by a simple linear operation, thereby indicating that the two equation systems are not linearly independent. As a consequence it is not possible to obtain a solution using the new equation system formulation since the equations for x_7 and x_8 are essentially redundant. Thus the only procedure considered applicable is to use the original system as a means of determining the force coefficients C_M and C_D, with the understanding that any effects of a current will be determined as a parametric dependency in the coefficient values. Such a result, when accompanied by good matching of the experimental measurements together with an indicated set of constant coefficients, shows that the Morison equation model would be valid for the case of a current combined with wave disturbances. However, it would be expected that the influence of the current would manifest itself in possibly altering the coefficient values as compared to the case when no current was present, but that will have to be determined by means of data analysis applied to the results obtained following the identification procedure.

DIMENSIONAL ANALYSIS OF FORCE COEFFICIENTS

The system identification procedure described previously will be applied to determine the numerical values of the force coefficients in the Morison equation model, for each case that is considered. However there is no indication of the basic dependency of such coefficients on various physical parameters that characterize the general flow phenomena, when using that method. The most useful means of determining the dependence of the force coefficients on various physical parameters is by the use of dimensional analysis, which will indicate the dependence on various sets of dimensionless parameters that have been evidenced in other studies of wave forces on offshore structures.

As an initial simple illustration, the case of a single in-line resultant velocity approaching a cylindrical vertical element structure is considered. The force is represented by the relation

$$F = C_M \frac{\rho \pi D^2}{4} L\dot{u} + C_D \frac{\rho}{2} DLu|u| \qquad (31)$$

where L is the length of the cylindrical element and all of the other terms have been generally defined previously. The physical parameters on which the force depends are listed below: u_o, u, D, ρ, μ, T, H, g, ε, where

u_o = current velocity

u = wave velocity

μ = fluid viscosity

T = wave period

H = wave height

g = gravity acceleration

ε = roughness size

Considering a product form of representation for each component term of the force expression in Eq. (31) leads to the expression

$$C_M \frac{\rho \pi D^2}{4} L\dot{u} = K u_o^a u^b D^c \rho^d \mu^e T^f H^g g^h \varepsilon^i \qquad (32)$$

for the inertial component of the force, where K is a constant. Using the basic dimensions of force, length and time (F,L,T system) for each physical parameter on the right hand side of Eq. (32) results in three basic equations for the different powers of the basic dimensional quantities (F, L, and T). These equations are:

$$\begin{aligned} 1 &= d+e \\ 0 &= a+b+c+g+h+i-4d-2e \\ 0 &= 2d+e+f-a-b-2h \end{aligned} \tag{33}$$

Combining these equations lead to relations in terms of a reduced number of variables, which then result in the expression

$$C_M \frac{\rho\pi D^2}{4} L\dot{u} = K \cdot \rho u^2 D^2 \left(\frac{u_o}{u}\right)^a \left(\frac{\mu}{\rho D u}\right)^e \left(\frac{uT}{D}\right)^f \left(\frac{H}{D}\right)^g \left(\frac{gD}{u^2}\right)^h \left(\frac{\varepsilon}{D}\right)^i \tag{34}$$

or

$$C_M = K_1 \frac{u^2}{L\dot{u}} \left(\frac{u_o}{u}\right)^a (Re)^{-e} (KC)^f \left(\frac{H}{D}\right)^g (Fr)^{-h} \left(\frac{\varepsilon}{D}\right)^i \tag{35}$$

where

K_1 is a constant

$Re = \frac{\rho Du}{\mu}$ = Reynolds number

$KC = \frac{uT}{D}$ = Keulegan-Carpenter number

$Fr = \frac{U^2}{gD}$ = Froude number

The functional representation for the inertia coefficient C_M is then given by the expression

$$C_M = \frac{u^2}{L\dot{u}} f_1 \left(\frac{u_o}{u}, Re, KC, \frac{H}{D}, Fr, \frac{\varepsilon}{D}\right) \tag{36}$$

where the initial functional coefficient $\frac{u^2}{L\dot{u}}$ is some type of "Froude number" based on the fluid acceleration, $\frac{H}{D}$ is an alternate representation of the KC number (evaluated at the free surface), and $\frac{\varepsilon}{D}$ is a measure of the relative roughness.

The analysis of the drag force component then follows from the basic relation

$$C_D \frac{\rho}{2} DLu|u| = K u_o^a u^b D^c \rho^d \mu^e T^f H^g g^h \epsilon^i \qquad (37)$$

which yields the following equations for the powers of the three fundamental physical variables (FLT); viz.

$$\begin{aligned} 1 &= d+e \\ 0 &= a+b+c-4d-2e+g+h+i \\ 0 &= -a-b+2d+e+f-2h \end{aligned} \qquad (38)$$

Combining these relations and establishing the pertinent dimensionless parameter quantities results in

$$C_D = \frac{D}{L} f_2\left(\frac{u_o}{u}, Re, KC, \frac{H}{D}, Fr, \frac{\epsilon}{D}\right) \qquad (39)$$

As a result of the dimensional analysis shown here, the force coefficients C_M and C_D from the Morison equation model are shown to be functions of the ratio of the current magnitude to the wave velocity amplitude; the Reynolds number; the Keulegan-Carpenter number; the Froude number; the ratio of wave height to diameter; and the relative roughness ratio. The particular functional form is not specified, nor is the degree of dependence on each dimensionless parameter indicated. However, this basic dependence on these specific parameters will allow some means of plotting the numerical values obtained from the system identification analysis in a form that would exhibit some type of consistent variation, assuming that such a consistent dependence was exhibited by the data.

If the basic mathematical model was represented in the form

$$F = C_M \frac{\rho \pi D^2}{4} \dot{u} + C_D \frac{\rho}{2} DL(u_o+u)|u_o+u| \qquad (40)$$

the same relation as Eq. (36) would be found for the inertia coefficient C_M. The equation for the drag coefficient C_D would be similar to that in Eq. (39) except for an additional multiplying constant of the form

$$\frac{u^2}{(u_o+u)|u_o+u|} \qquad (41)$$

which can be seen to just be an additional manifestation of the dependence on the parameter $\frac{u_o}{u}$. Thus, even if the basic force equation was represented in the form of Eq. (40) to include the presence of the current in a direct manner, the basic functional dependence of the drag coefficient C_D would not be altered in a significant manner.

In the present case of two component wave velocities in the horizontal plane, for a vertical leg element of length L, the Morison force equations are represented by Eq. (16) - (18) with the inclusion of the multiplying length factor L. The same type of dimensional analysis procedure can be applied to that model, where the basic physical variables are expanded to include the separate component terms such as u_{x_o}, u_{y_o}, u_x, u_y, etc.

Considering the x-component force expression, for the inertial force portion initially, the same type of dimensional analysis procedure leads to the relation

$$C_M = \frac{u_x^2}{L\dot{u}_x} f_3\left(\frac{u_{x_o}}{u_x}, \frac{u_{y_o}}{u_x}, \frac{u_y}{u_x}, Re_x, KC_x, \frac{H}{D}, Fr_x, \frac{\varepsilon}{D}\right) \qquad (42)$$

where Re_x, KC_x, and Fr_x are defined in terms of the velocity component u_x. The drag force component of the x-force can be shown to be represented by

$$C_D = \frac{u_x}{u_x^2 + u_y^2} \frac{D}{L} f_4\left(\frac{u_{x_o}}{u_x}, \frac{u_{y_o}}{u_x}, \frac{u_y}{u_x}, Re_x, KC_x, \frac{H}{D}, Fr_y, \frac{\varepsilon}{D}\right) \qquad (43)$$

Applying these same methods to the y-component force results in

$$C_M = \frac{u_y^2}{L\dot{u}_y} f_5\left(\frac{u_{x_o}}{u_y}, \frac{u_{y_o}}{u_y}, \frac{u_x}{u_y}, Re_y, KC_y, \frac{H}{D}, Fr_y, \frac{\varepsilon}{D}\right) \qquad (44)$$

and

$$C_D = \frac{u_y}{u_x^2 + u_y^2} f_6\left(\frac{u_{x_o}}{u_y}, \frac{u_{y_o}}{u_y}, \frac{u_x}{u_y}, Re_y, KC_y, \frac{H}{D}, Fr_y, \frac{\varepsilon}{D}\right) \qquad (45)$$

where Re_y, KC_y, and Fr_y are defined in terms of the velocity component u_y.

A reduction in the parameters for the dependency of the inertia and drag coefficients can be achieved by means of applying physical reasoning as well as other simple relationships. Since these force coefficients should not be dependent only on the component of velocity associated with the particular direction of the force from which the basic relationship was obtained, the basic dependence is really exhibited in terms of resultant velocity quantities. However there is also an indicated dependence on the ratio $\frac{u_x}{u_y}$. In addition the quantity $\frac{u^2}{L\dot{u}}$ (or its inverse) can be represented, by means of the relation $\dot{u} \sim \frac{u}{T}$ which is applicable to a purely oscillatory function (in terms of the amplitudes of the respective quantities), so that $\frac{u^2}{L\dot{u}} \sim \frac{uT}{L}$ which is another type of Keulegan-Carpenter number.

On the basis of the above reasoning it can be seen that the Morison equation force coefficients are generally a function of the following parameters:

$$Re,\ KC,\ Fr,\ \frac{H}{D},\ \frac{D}{L},\ \frac{\varepsilon}{D},\ \frac{u_o}{u},\ \frac{u_x}{u_y}$$

with the first three quantities defined in terms of the resultant velocity (as in the definitions following Eq. (35) above). Some of these parameters can also be combined further to reflect the dependence on the parameter $\beta=Re/KC$, which has been used as a basic dimensionless parameter for many wave force investigations (e.g. see [3]). Another relation that is possible is the parameter defined by

$$\frac{u_o}{u}KC = \frac{u_o T}{D} = V_R \qquad (46)$$

which is the Verley-Moe coefficient reflecting the influence of the current present together with an oscillatory flow (see [17]).

The dimensional analysis procedure described above outlines the basic parameter dependency that may be exhibited by the coefficients determined in the present investigation. The degree of dependence of those resulting coefficients will be exhibited in terms of some of these quantities in order to gain insight and understanding regarding their possible use for conditions other than those from the data set that was used in this study.

RESULTS OBTAINED AND DISCUSSION

The system identification procedure described previously in earlier sections was applied to the various 27-30 second records selected for analysis. These records were C-1 through C-38 from the C wave group of separate wave segments; a group of 124 records (27 seconds long, each) obtained from the total wave record tape LS8A; and a group of sixty 27 second long records selected from wave record tape SS9. The C wave records and those from LS8A were obtained from measurements of both the wave velocities and the forces at a vertical leg element (at 15 ft. depth) of the NW leg of the OTS, which was painted with anti-fouling paint. The records from SS9 contained force measurements at the SW leg of the OTS (an unpainted element), with the velocities measured at the SE leg and transported via mathematical operations reflecting the proper phase shift properties according to the procedure described in [9].

As was discussed in an earlier section, the method of analysis used for measured data where a current may be present is the same as that for the case with no current (i.e. [15]). The only differences due to the current influence would be manifested in a parametric manner for the coefficients, and that will have to be determined from an analysis of the Morison equation force coefficients in regard to their dependence on various dimensionless parameters.

Representative examples of the correspondence between the measured data and the estimated results obtained by the system identification procedure applied to the present data set are shown in Figures 6-9, where the instantaneous C_M and C_D values are used to calculate the estimated forces. The values of these coefficients, which are essentially constant throughout the 27-30 second time extent of each record, are also illustrated in these figures. These results are essentially similar in nature to those found in [15] and [9], with good "tracking" of the measured velocities and forces by the estimates from the identification procedure together with constant force coefficients. Thus the present system identification technique, when applied to determine the Morison equation force coefficients for cases where a current is present, can also provide valid results for such cases.

In the present case a definition for the Reynolds number (Re) and Keulegan-Carpenter number (KC) is established for any wave record in terms of the average value of the maximum resultant velocity for the trough and crest of the velocity. These parameters are calculated from the relations

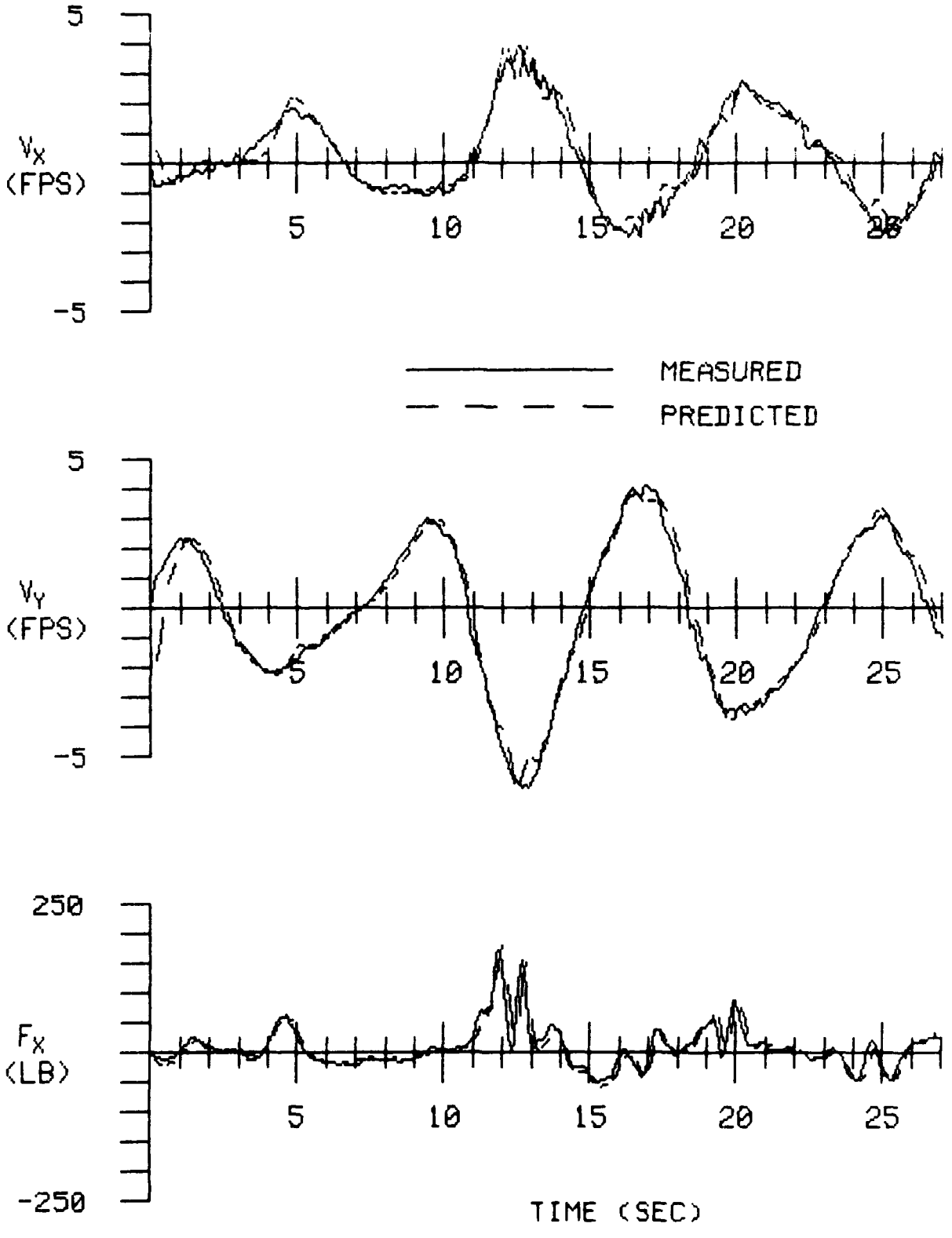

Fig. 6 Comparison of measured and predicted variables, and illustration of related quantities for system identification, C-18 wave.

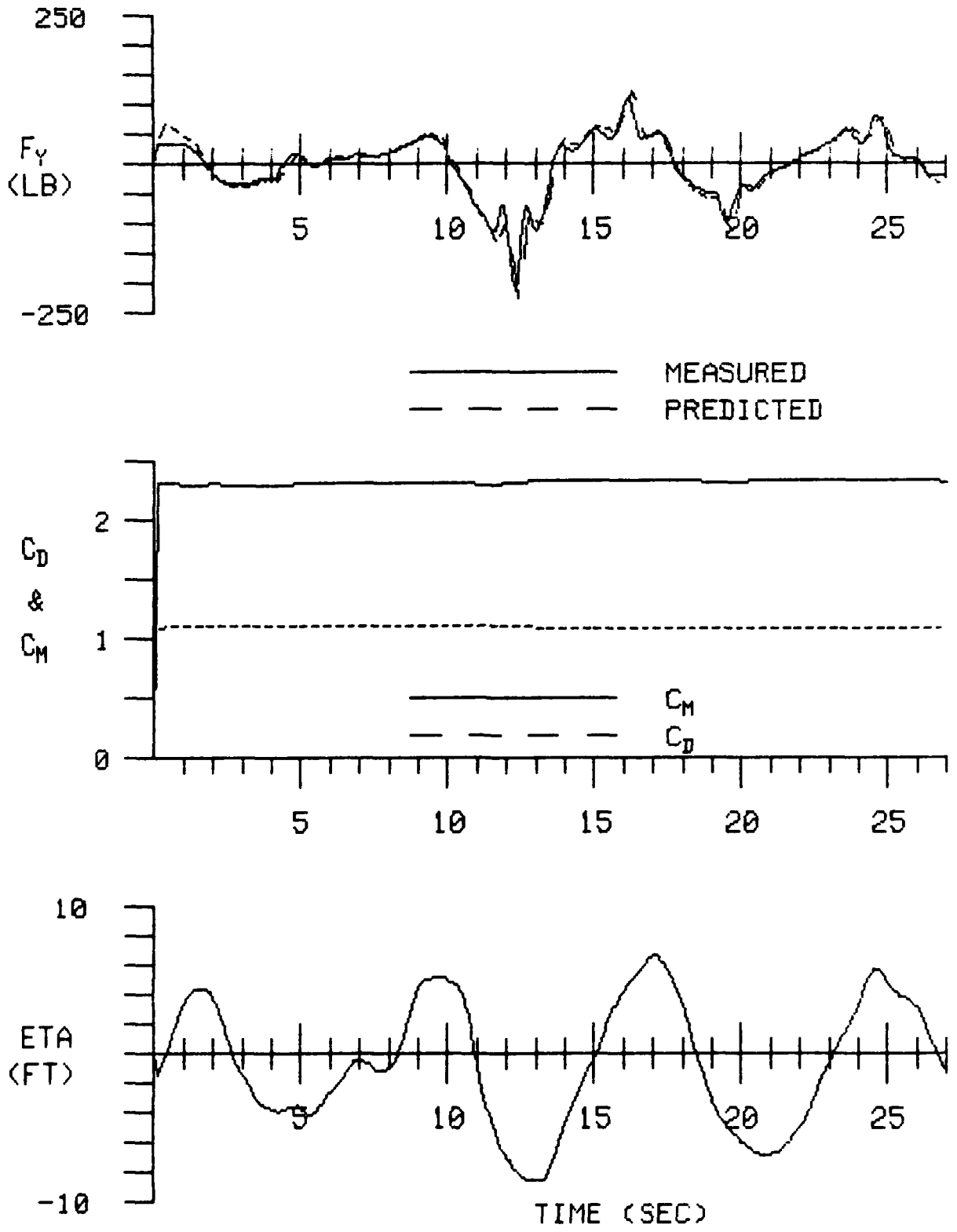

Fig. 6 (Continued)

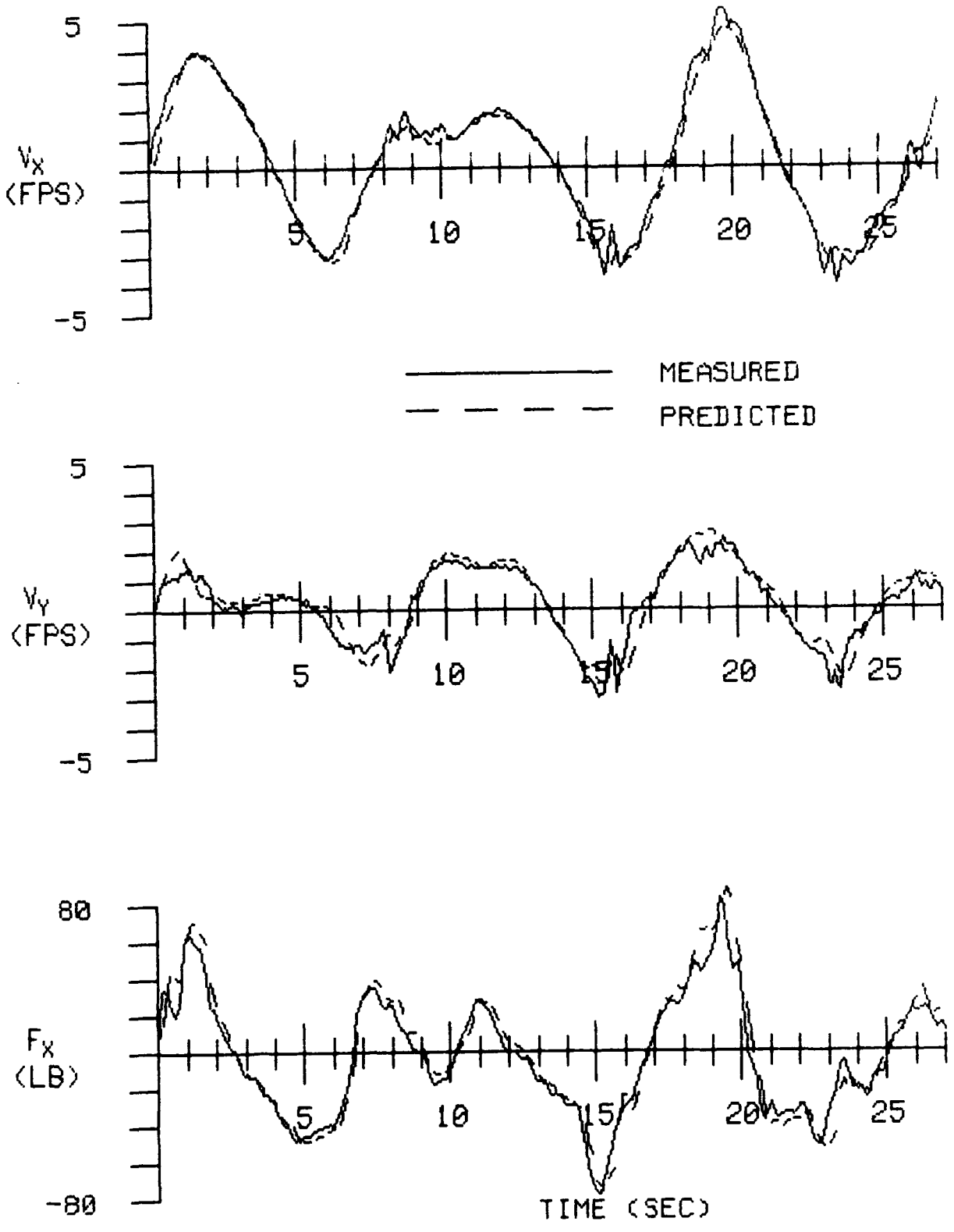

Fig. 7 Comparison of measured and predicted variables, and illustration of related quantities for system identification, C-34 wave.

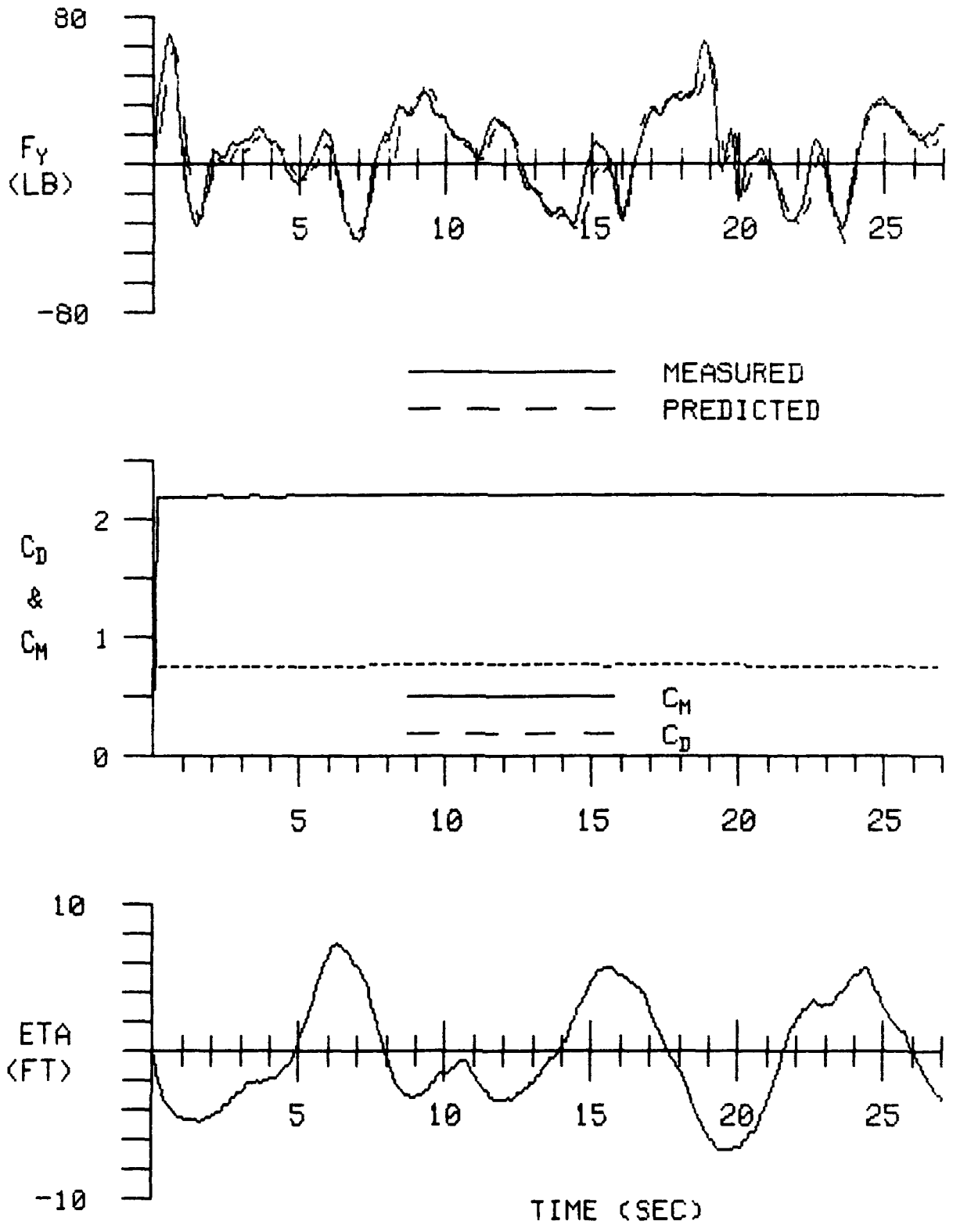

Fig. 7 (Continued)

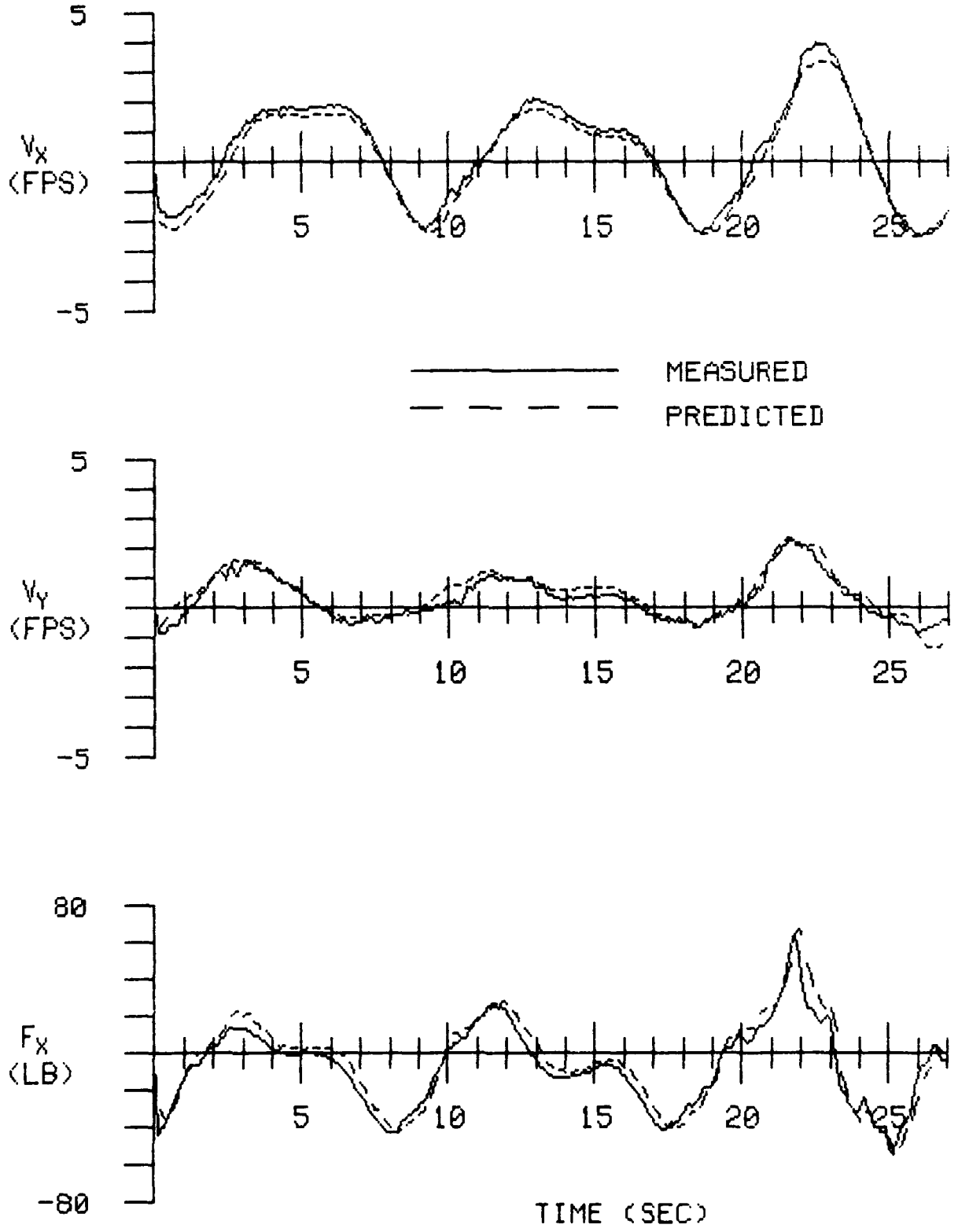

Fig. 8 Comparison of measured and predicted variables, and illustration of related quantities for system identification, LS8A wave segment 60.

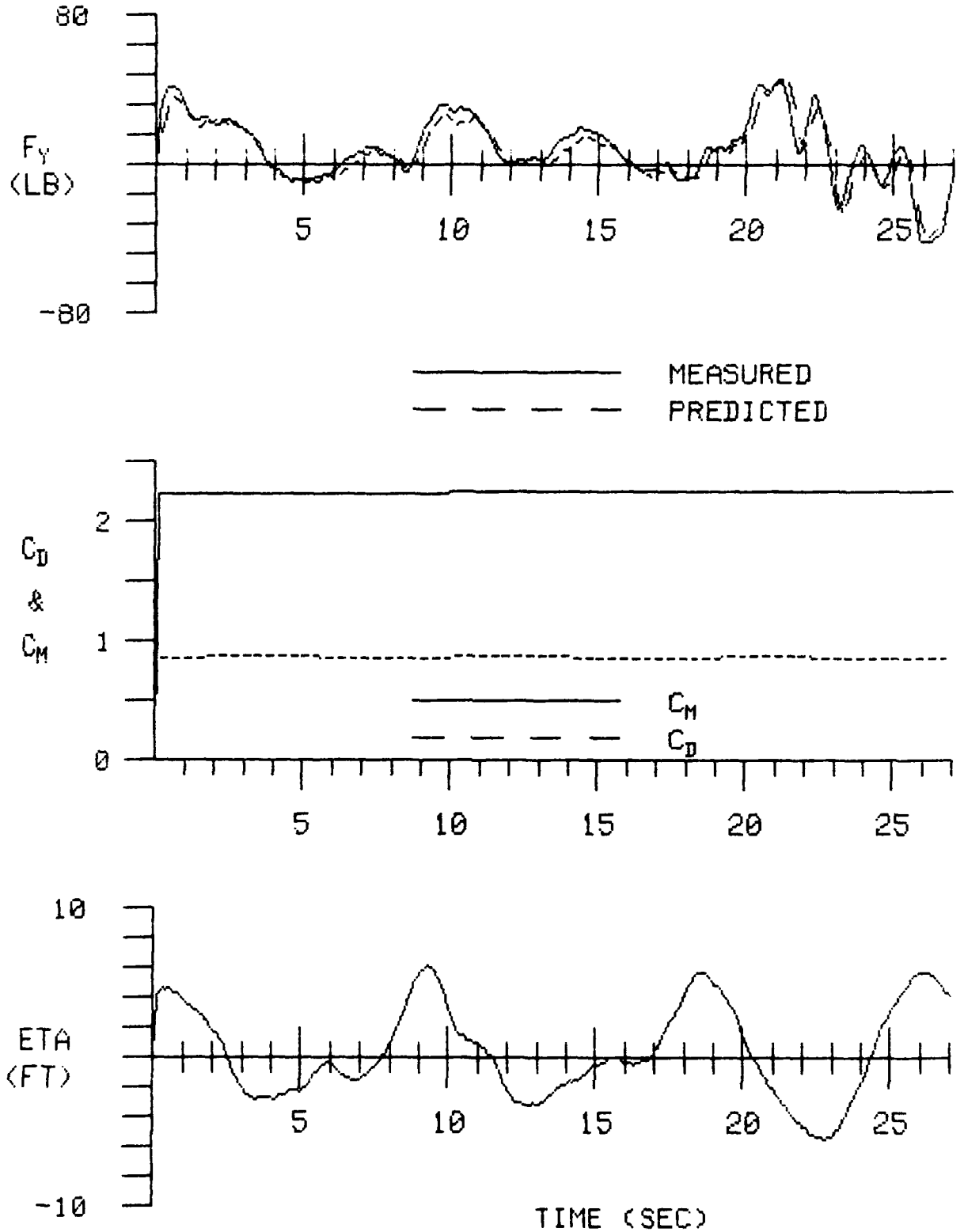

Fig. 8 (Continued)

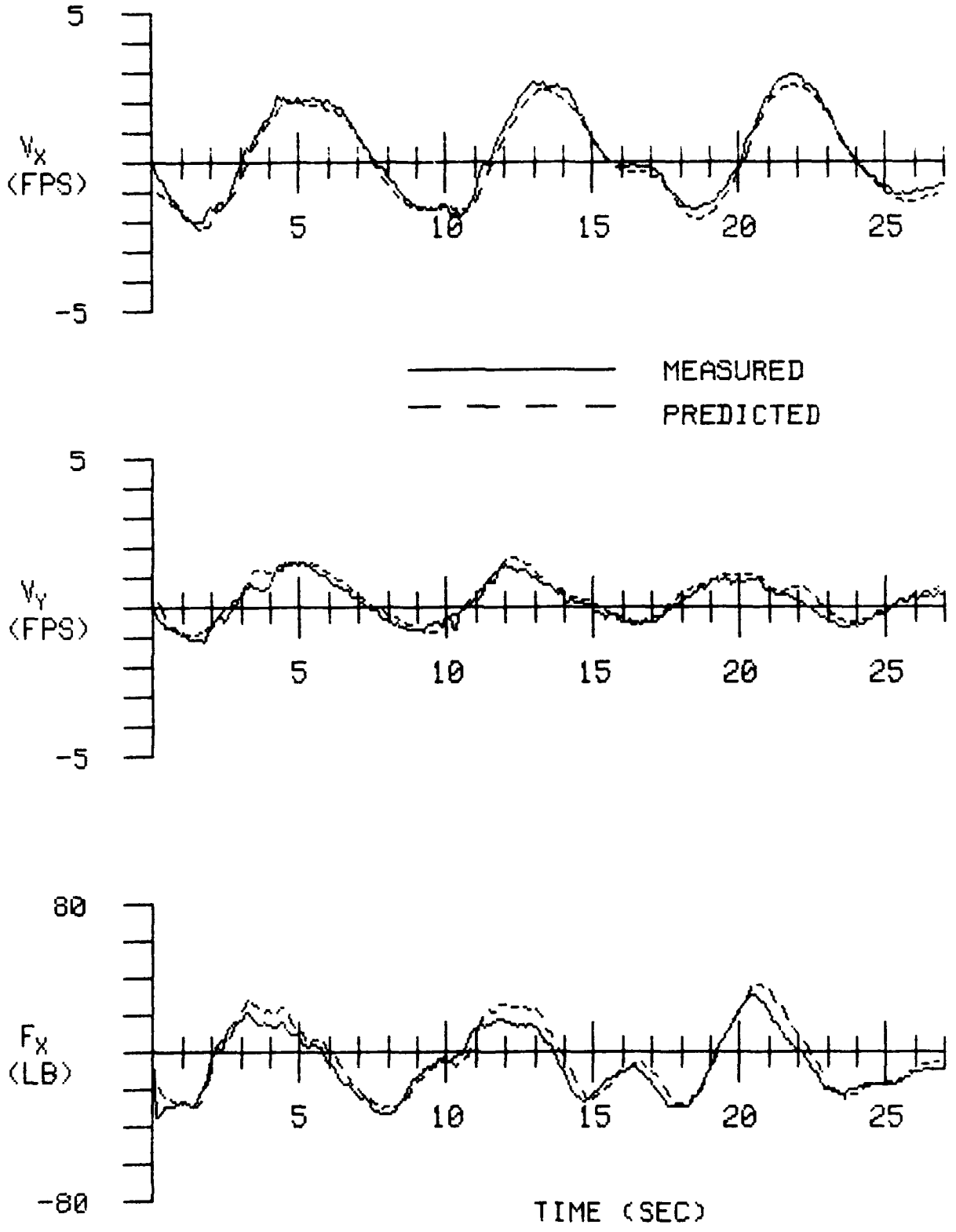

Fig. 9 Comparison of measured and predicted variables, and illustration of related quantities for system identification, LS8A wave segment 75.

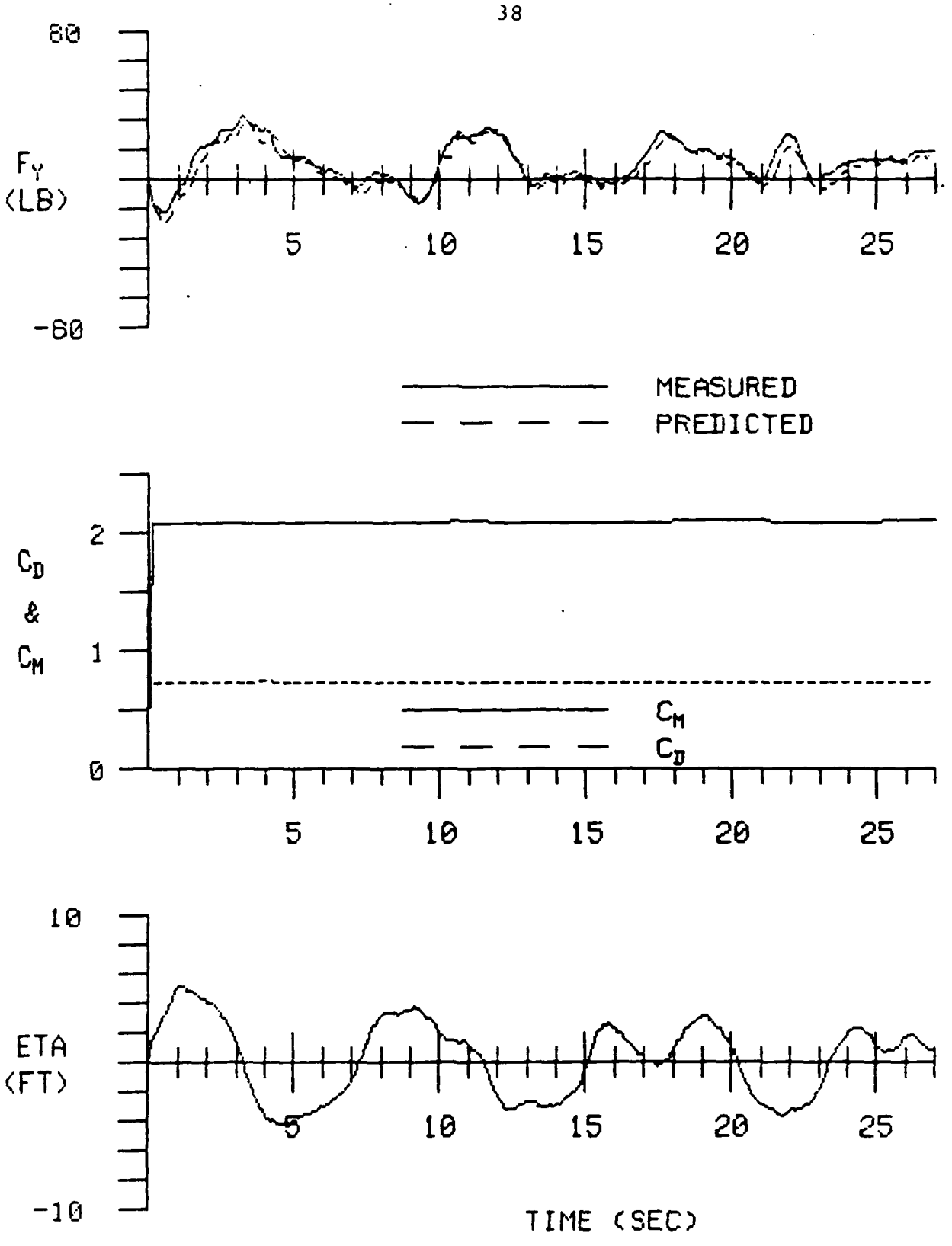

Fig. 9 (Continued)

$$Re = \frac{1}{2}\frac{D}{\nu}\left[(u_{trough})_{max} + (u_{crest})_{max}\right] \qquad (47)$$

$$KC = \frac{1}{2}\frac{T}{D}\left[(u_{trough})_{max} + (u_{crest})_{max}\right] \qquad (48)$$

These definitions are used in order to present variations of the force coefficients C_M and C_D as functions of these basic dimensionless reference numbers, which can also be contrasted with the results obtained in other studies (if desired).

Tabulations of the result for the force coefficients C_M and C_D found by application of the present system identification technique are given in Tables 1-3, which present the force coefficient values and related parameter values for each of the wave data groups analyzed here (C-waves, LS8A, and SS9). Included in these parameters are the ratio of the current velocity to the wave velocity, where the wave velocity is the average value defined in Eqs. (47) and (48) in terms of trough and crest values. The current value, denoted as u_o, is the resultant current, just as the wave velocity is the resultant wave velocity defined in Eq. (18). There is no dependence on any angular effects due to the lack of any direction dependence for each of these velocity quantities. Thus the effect of the dominant angle of wave propagation is not manifested in any manner in the present results.

The resultant current magnitude for the C-waves ranges from .04-.19 ft./sec. (with only 2 wave segments having that larger current value within the 38 C-wave records), while the current for the LS8A waves is .17 ft./sec. for all of the wave segments. The current magnitude is much larger for the SS9 wave segments, with a value of .77 ft./sec. applying to all of those records. The current values were found from available hourly summary tape records from the OTS records for the C-waves, where these hourly summary values are mean values obtained from 20 minutes averages found every hour during the data-recording time. The current values for the LS8A and SS9 wave segments were found as the mean values of the respective one hour record for each case.

In order to illustrate the variation of the force coefficients C_M and C_D with different parameters, some graphs showing

TABLE 1

Force Coefficient Values Obtained From System Idenfication Procedure

(C-waves, NW corner, painted sensor)

Wave	$Re \times 10^{-5}$	KC	$\beta \times 10^{-3}$	C_M	C_D	u_o/u	V_R
C-1	4.97	18.3	27.2	2.11	1.46	.017	.31
C-2	3.84	13.6	28.2	2.14	1.59	.023	.31
C-3	3.84	15.3	25.1	2.08	1.55	.023	.35
C-4	4.68	17.7	26.4	2.07	1.26	.018	.32
C-5	3.57	13.0	27.5	2.06	1.50	.024	.31
C-6	4.97	21.5	23.1	1.97	1.30	.017	.37
C-7	4.02	14.9	27.0	1.95	1.25	.012	.18
C-8	5.74	25.3	22.7	2.14	1.23	.009	.23
C-9	4.55	16.7	27.2	2.05	1.15	.011	.18
C-10	4.90	22.1	22.2	1.92	1.13	.010	.22
C-11	3.76	15.8	23.8	2.10	1.35	.013	.21
C-12	4.02	21.8	18.4	2.05	1.36	.031	.68
C-13	4.51	21.9	20.6	2.06	1.19	.027	.59
C-14	3.60	12.1	29.8	2.05	1.32	.033	.40
C-15	4.88	22.8	21.4	2.09	1.07	.025	.57
C-16	4.88	19.3	25.3	2.08	1.08	.025	.48
C-17	4.84	24.9	19.4	2.00	1.10	.028	.70
C-18	7.16	32.6	22.0	2.30	1.08	.019	.62
C-19	5.13	26.2	19.6	2.14	1.05	.024	.63
C-20	6.13	28.2	21.7	1.92	.88	.022	.62
C-21	5.82	17.9	32.5	2.03	1.26	.023	.41
C-22	6.14	29.7	20.7	1.91	.93	.022	.65
C-23	6.14	28.5	21.5	1.85	.94	.022	.63
C-24	7.4	38.5	19.2	2.26	.88	.018	.69
C-25	5.64	27.9	20.2	1.97	.99	.042	1.17
C-26	5.25	27.3	19.2	2.15	1.04	.045	1.23
C-27	6.16	33.6	18.3	2.11	.86	.024	.81
C-28	26.3	32.3	19.3	2.24	1.05	.024	.78
C-29	7.04	39.1	18.0	2.36	.87	.021	.82
C-30	6.46	36.3	17.8	2.03	.74	.023	.83
C-31	5.95	32.9	18.1	2.04	.74	.025	.82
C-32	6.05	26.6	22.7	2.16	.77	.025	.67
C-33	5.75	23.2	24.8	2.18	.86	.026	.60
C-34	6.56	32.8	20.0	2.19	.75	.023	.75
C-35	5.59	31.5	17.7	2.17	.91	.026	.82
C-36	8.08	40.6	19.9	2.46	.84	.018	.73
C-37	7.97	44.3	18.0	2.55	.96	.018	.80
C-38	6.23	35.0	17.8	2.45	1.15	.024	.84

TABLE 2

Force Coefficient Values Obtained From System Idenfication Procedure

(LS 8A waves, NW corner, painted sensor)

Wave	$Re \times 10^{-5}$	KC	$\beta \times 10^{-3}$	C_M	C_D	u_o/u	V_R
001	2.17	10.1	21.5	2.09	1.00	.097	.98
002	3.50	12.8	27.3	2.14	0.88	.060	.77
003	2.12	7.4	28.6	2.23	1.39	.10	.74
004	1.52	6.0	25.3	2.18	1.08	1.39	.83
005	3.37	11.6	29.1	2.24	1.38	.063	.73
006	2.99	16.9	17.7	2.16	.97	.071	1.2
007	2.53	7.1	35.6	2.22	1.09	.083	.59
008	2.34	10.1	23.2	2.18	1.13	.090	.91
009	2.19	6.93	31.6	2.13	1.33	.096	.67
010	2.92	24.8	11.8	2.14	.93	.072	1.79
011	5.89	30.1	19.6	2.26	.84	.036	1.08
012	2.59	9.8	26.4	2.35	1.14	.081	.79
013	2.49	12.9	19.3	2.26	1.03	.085	1.10
014	3.3	17.1	19.3	2.18	.96	.064	1.09
015	2.31	9.7	23.8	2.15	1.30	.091	.88
016	2.97	17.4	17.1	2.11	.90	.071	1.21
017	2.46	10.9	22.6	2.21	1.05	.086	.94
018	5.6	27.8	20.1	2.12	1.07	.038	1.06
019	4.02	21.3	18.0	2.11	1.02	.052	1.16
020	2.78	13.9	20.0	2.18	1.20	.076	1.06
021	2.57	11.2	22.2	2.17	1.04	.082	.92
022	3.29	17.2	19.1	2.28	.81	.062	1.10
023	3.73	20.8	17.9	2.13	.97	.057	1.19
024	3.40	18.3	18.6	2.23	.99	.062	1.13
025	2.26	11.1	20.4	2.20	1.16	.093	1.03
026	3.24	16.1	20.1	2.15	.77	.065	1.05
027	4.32	19.0	22.7	2.17	.87	.049	.93
028	2.76	14.1	19.6	2.11	.84	.076	1.07
029	3.46	16.0	21.6	2.31	1.23	.061	.98
030	2.36	8.2	28.8	2.28	1.23	.098	.73
031	1.91	6.0	31.8	2.25	1.33	.11	.66
032	4.07	15.9	25.6	2.20	1.03	.052	.83
033	2.30	8.2	28.0	2.18	1.06	.092	.75
034	3.12	12.8	24.4	2.14	.99	.068	.87
035	3.51	18.3	19.2	2.13	.82	.060	1.10
036	2.71	12.8	21.2	2.13	1.00	.078	1.0
037	2.07	7.4	28.0	2.18	1.28	.102	.75
038	2.28	10.9	20.9	2.17	1.00	.093	1.01
039	3.17	15.4	20.6	2.23	1.11	.067	1.03
040	2.45	9.9	24.7	2.22	.95	.086	.85
041	3.22	15.9	20.3	2.13	.96	.066	1.05
042	2.84	13.3	21.4	2.16	1.07	.074	.98
043	4.9	24.1	20.3	2.24	.94	.043	1.04
044	2.94	12.3	23.9	2.12	.89	.072	.89
045	2.46	10.7	23.0	2.16	.82	.086	.92

TABLE 2 (continued)

Wave	$Re \times 10^{-5}$	KC	$\beta \times 10^{-3}$	C_M	C_D	u_o/u	V_R
046	2.56	10.4	24.6	2.12	.88	.082	.85
047	2.31	8.5	27.2	2.19	1.04	.091	.77
048	2.98	11.0	27.1	2.12	.99	.071	.78
049	2.99	14.6	20.5	2.13	.99	.071	1.04
050	4.42	16.7	26.5	2.08	.95	.048	.80
051	2.43	9.4	25.9	2.25	1.18	.087	.82
052	1.92	6.5	29.5	2.05	1.02	.110	.72
053	4.14	20.1	20.7	2.32	1.68	.051	1.03
054	3.38	21.5	15.7	2.24	1.08	.062	1.33
055	3.76	17.6	21.4	2.10	1.00	.056	.99
056	3.70	17.9	20.7	2.04	1.01	.057	1.02
057	1.46	7.2	20.3	2.21	1.20	.145	1.04
058	2.96	16.2	18.3	2.26	1.03	.086	1.39
059	3.33	15.4	21.6	2.17	1.00	.063	.97
060	4.25	22.5	18.9	2.24	.86	.050	1.13
061	3.56	18.4	19.3	2.20	.89	.059	1.09
062	2.98	12.9	23.1	2.16	.88	.071	.92
063	2.42	10.1	24.0	2.10	1.20	.087	.88
064	3.97	18.5	21.5	2.11	.96	.053	.98
065	2.48	11.0	22.5	2.14	1.08	.085	.94
066	3.39	15.2	22.3	2.08	.92	.062	.94
067	2.78	10.3	27.0	2.22	.89	.076	.93
068	3.09	11.9	26.0	2.14	.73	.068	.81
069	2.42	9.7	30.1	2.10	1.00	.072	.70
070	3.21	11.4	28.2	2.19	1.07	.066	.75
071	4.21	15.5	27.2	2.10	.93	.050	.78
072	3.87	16.2	23.9	2.08	.90	.055	.89
073	2.69	10.2	26.4	2.15	.90	.078	.80
074	3.44	18.3	18.8	2.10	.70	.061	1.12
075	3.22	15.7	20.5	2.09	.72	.066	1.04
076	4.31	21.9	19.7	2.18	.62	.049	1.07
077	1.9	6.8	27.9	2.09	.68	.111	.75
078	2.58	9.0	28.7	2.17	.92	.082	.74
079	3.14	15.6	20.1	2.04	.57	.067	1.05
080	1.63	6.4	25.5	2.19	1.05	.129	.83
081	4.35	21.8	20.0	2.18	.97	.049	1.07
082	2.27	9.2	24.7	2.20	1.04	.093	.86
083	3.28	16.0	20.5	2.11	.85	.064	1.02
084	3.85	18.9	20.4	2.04	.84	.055	1.04
085	2.82	9.2	30.7	2.24	1.25	.075	.69
086	2.41	13.4	18.0	2.15	1.04	.088	1.18
087	2.76	11.5	24.0	2.05	.71	.076	.87
088	2.61	9.2	28.4	2.18	.68	.081	.75
089	1.73	6.7	25.8	2.22	.95	.122	.82
090	2.80	12.6	22.2	2.19	1.06	.075	.95
091	3.54	19.4	18.2	2.28	.94	.060	1.16
092	2.55	11.8	21.6	2.08	.88	.083	.98
093	3.39	10.8	30.6	2.10	.75	.064	.69
094	4.12	20.5	20.1	2.05	.62	.051	1.05
095	3.52	13.9	25.3	2.21	.86	.060	.83

TABLE 2 (continued)

Wave	$Re \times 10^{-5}$	KC	$\beta \times 10^{-3}$	C_M	C_D	u_o/u	V_R
096	2.10	7.1	29.6	2.17	1.02	.100	.71
097	1.98	6.6	3.0	2.18	.87	.107	.71
098	2.36	8.2	28.8	2.03	.71	.089	.73
099	2.16	10.0	21.6	2.09	.97	.098	1.18
100	3.22	16.3	19.8	2.19	.96	.066	1.08
101	4.17	20.9	20.0	2.18	.90	.051	1.07
102	6.65	33.3	20.0	2.00	.64	.032	1.07
103	2.75	10.5	26.2	2.12	.95	.077	.81
104	2.01	7.3	27.5	2.23	1.02	.105	.77
105	2.77	12.0	23.1	2.16	.76	.076	.91
106	2.50	7.8	32.1	2.12	.71	.084	.66
107	3.15	16.0	19.7	2.26	.96	.067	1.07
108	2.48	7.7	32.2	2.24	.89	.085	.65
109	3.49	15.2	23.0	2.19	.95	.060	.91
110	2.40	10.3	23.3	2.19	.74	.088	.91
111	2.37	14.2	16.7	2.16	.90	.089	1.26
112	3.22	17.0	18.9	2.12	1.04	.066	1.12
113	5.77	25.6	22.5	2.24	.87	.037	.95
114	3.62	18.2	19.9	2.23	.96	.058	1.06
115	4.10	24.5	16.7	2.15	.85	.051	1.25
116	3.78	17.8	21.2	2.25	.84	.056	1.00
117	2.07	10.5	19.7	2.19	.78	.102	1.07
118	3.40	17.6	19.3	2.15	.77	.062	1.09
119	2.46	7.9	31.1	2.20	.98	.086	.68
120	1.74	6.9	25.2	2.18	.76	.121	.83
121	1.36	3.6	37.8	2.18	1.00	.155	.56
122	3.25	17.3	18.8	2.14	.87	.106	1.12
123	3.2	12.2	26.2	2.18	.68	.066	.81
124	2.6	16.4	15.9	1.99	.61	.081	1.33

TABLE 3

Force Coefficient Values Obtained From System Idenfication Procedure

(SS9 waves, SW corner, unpainted sensor)

Wave	$Re \times 10^{-5}$	KC	$\beta \times 10^{-3}$	C_M	C_D	u_o/u	V_R
01	3.21	16.9	19.0	2.02	1.39	.296	5.0
02	3.70	20.96	17.7	2.34	1.25	.257	5.4
03	2.75	14.9	18.5	2.13	1.32	.346	5.2
04	2.87	16.5	17.4	2.14	1.21	.331	5.5
05	3.0	13.8	21.7	2.26	1.80	.317	4.4
06	3.05	14.4	21.2	2.56	1.75	.310	4.5
07	6.11	31.5	19.4	2.46	1.5	.156	4.9
08	2.80	16.9	16.6	2.28	.85	.338	5.7
09	2.74	14.2	19.3	2.19	1.49	.347	4.9
10	2.8	12.1	23.1	2.12	.72	.341	4.1
11	2.82	17.8	15.8	2.10	1.01	.336	6.0
12	3.34	17.7	18.9	2.15	.96	.285	5.0
13	3.05	15.6	19.6	1.98	1.19	.311	4.9
14	3.16	24.2	13.1	2.39	2.40	.300	7.3
15	3.06	16.1	19.0	2.29	1.46	.310	5.0
16	2.96	17.3	17.1	2.15	2.00	.321	5.6
17	3.14	16.2	19.4	2.33	1.48	.303	4.9
18	3.63	2.13	17.0	2.04	1.29	.262	5.6
19	4.80	27.6	17.4	2.13	1.52	.198	5.5
20	4.39	2.14	20.5	2.19	1.54	.219	4.7
21	3.55	17.2	20.6	2.10	1.52	.267	4.6
22	3.29	22.1	14.9	2.35	1.76	.289	6.4
23	4.79	27.8	17.2	2.51	1.56	.198	5.5
24	4.42	24.7	17.9	2.24	1.44	.215	5.3
25	3.72	22.0	16.9	2.14	1.24	.255	5.6
26	2.33	15.5	15.0	2.66	1.86	.408	6.3
27	2.79	19.1	14.6	2.2	1.32	.359	6.9
28	2.56	19.4	13.2	2.22	1.21	.371	7.2
29	2.75	11.3	24.3	2.12	1.35	.346	3.9
30	2.87	20.6	13.9	2.31	1.76	.331	6.8
31	2.78	14.6	19.0	2.14	1.70	.341	5.0
32	2.61	19.8	13.2	2.23	1.23	.364	7.2
33	2.81	29.1	9.7	2.12	1.68	.335	9.7
34	5.04	24.3	20.7	2.34	1.76	.188	4.6
35	2.49	19.8	12.6	2.20	1.50	.383	7.6
36	2.72	13.9	19.6	2.05	.98	.348	4.8
37	2.49	10.6	23.5	2.12	1.42	.382	4.0
38	2.85	14.5	19.7	2.18	1.18	.333	4.8
39	2.97	16.3	18.2	2.13	1.64	.320	5.2
40	1.85	12.0	15.4	2.14	1.34	.520	6.2

TABLE 3 (cont

Wave	$Re \times 10^{-5}$	KC	$\beta \times 10^{-3}$		C_D	u_o/u	V_R
41	3.65	18.0	20.3		1.46	.261	4.7
42	3.10	20.2	15.3		1.22	.307	6.2
43	2.79	13.6	20.5	2.07	1.26	.340	4.6
44	2.77	15.3	18.1	2.22	1.64	.343	5.2
45	3.08	18.2	16.4	2.07	1.20	.309	5.8
46	2.32	14.7	15.8	2.03	1.10	.410	6.0
47	2.57	10.5	24.5	2.06	1.12	.370	3.9
48	3.15	10.9	28.9	2.19	.185	.302	3.3
49	4.60	21.3	21.6	2.11	1.16	.207	4.4
50	2.20	12.3	17.9	2.03	1.48	.431	5.3
51	2.74	17.3	15.8	2.10	1.17	.348	6.0
52	2.23	15.5	14.4	2.16	1.48	.427	6.6
53	4.01	21.1	19.0	2.12	1.94	.237	5.0
54	2.3	13.7	16.8	2.14	1.14	.406	5.6
55	2.51	13.0	19.3	2.04	1.29	.380	4.9
56	2.88	14.2	20.3	2.15	1.08	.330	4.7
57	3.08	17.0	18.1	2.29	2.03	.309	5.3
58	2.79	10.1	27.6	2.15	1.25	.341	3.4
59	3.09	15.3	20.2	2.37	1.71	.306	4.7
60	3.44	17.5	19.7	2.40	1.92	.276	4.8

such variations have been prepared. The basic parameter chosen for grouping of results is the quantity β, which combines the effects of both Re and KC and has been shown to be a unifying quantity for grouping force values on structures in waves in other studies (e.g. [3]). The β-values have been grouped into the range 12-16,000 (with an average value of 14,000); 16-20,000 (with an average of 18,000); 20-24,000 (with an average of 22,000); and 24-28,000 (with an average of 26,000). There are some values outside these ranges, being both smaller and larger, but without enough data values to allow any proper grouping results.

The data from Tables 1 and 2 for the painted NW vertical leg element have been plotted with the abscissa being KC and the ordinate the particular force coefficient, for a particular β value representing the grouping described above, in Figures 10-12. The force values are also shown as functions of the ratio u_o/u, the ratio of current magnitude to the maximum wave velocity, by virtue of the different symbols defined in each figure which correspond to different ranges of this velocity ratio parameter.

Examination of these figures generally indicates that the drag coefficient C_D decreases with an increase in the current velocity ratio parameter u_o/u for each β value considered. However, there are limited regions of overlap in the KC values where such a definitive behavior is exhibited. This behavior is consistent with the results shown by Sarpkaya in [5]. The inertia coefficient C_M does not seem to indicate any significant variation with the current velocity, or with KC generally. The range of C_M values lies primarily between 2.0-2.25, with some lower and also higher values at the larger KC values (KC > 20-30). This behavior of C_M is consistent with the results of previous system identification analysis work for the OTS, as shown in [15] and [9], but differs from the values found by other methods such as in [2] and [6] where the values tend to be smaller (except for the inertia dominant range of low KC values).

Although there is some indication given by the data in Figures 10-12 (for the painted NW leg) that there is an influence of a current when present together with waves, the range of current values is too small there to indicate any definite trend with full acceptability. The results in [5] are certainly supportive, together with the general principle that the current will act to move the oscillatory wake further away from the cylindrical cross-section and thereby reduce the flow interaction and the resulting drag force. However more useful data to demonstrate the current influence is provided by the data set with larger current values, which was the basis for selecting the 60 waves from the SS9 record of the OTS investigation.

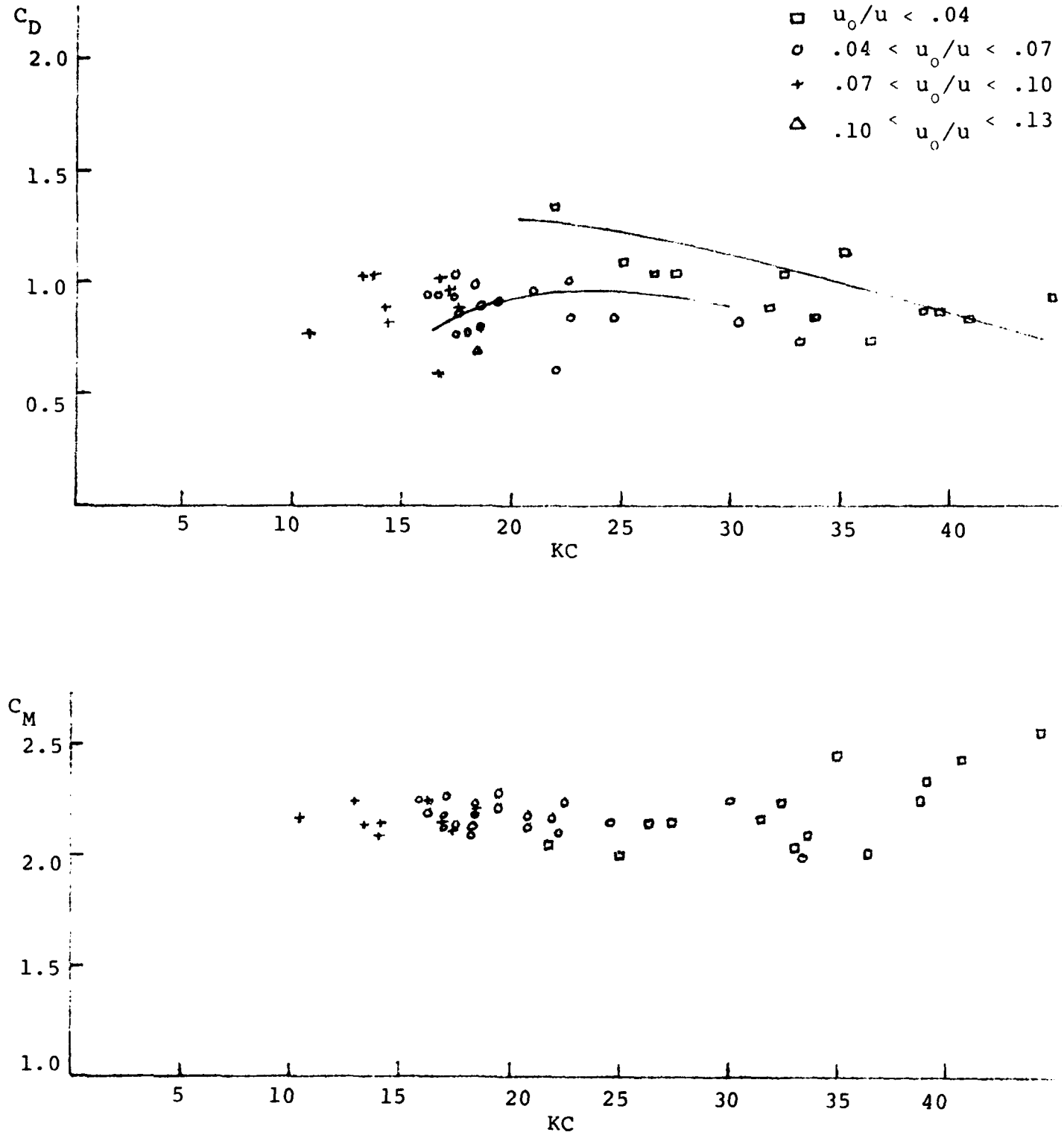

Fig. 10 C_D and C_M variation with KC, for different relative current values, C-waves and LS8A waves, NW (painted) element, $\beta \approx 18{,}000$ (average)

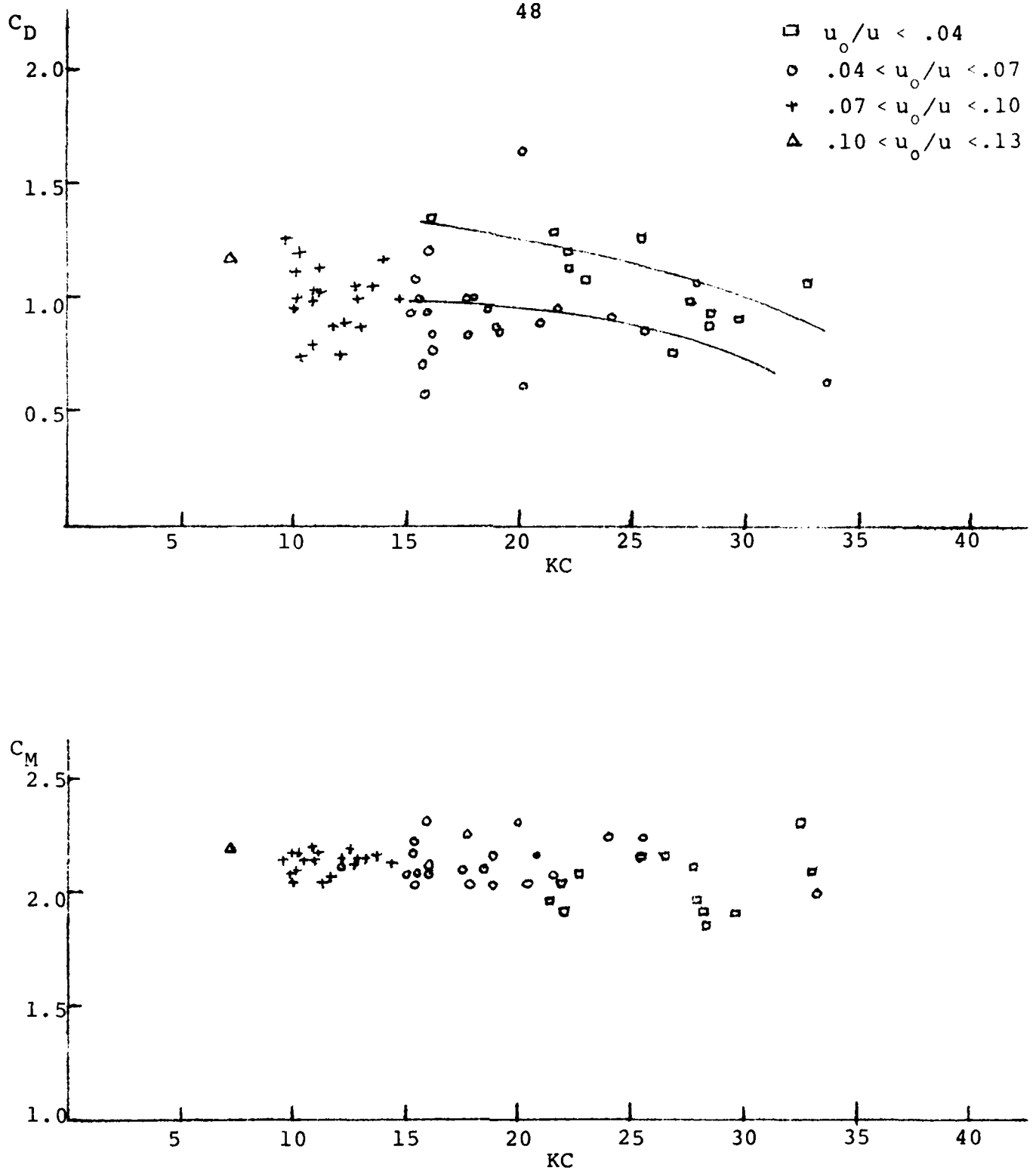

Fig. 11 C_D and C_M variation with KC, for different relative current values, C-waves and LS8A waves, NW (painted) element, $\beta \approx 22{,}000$ (average).

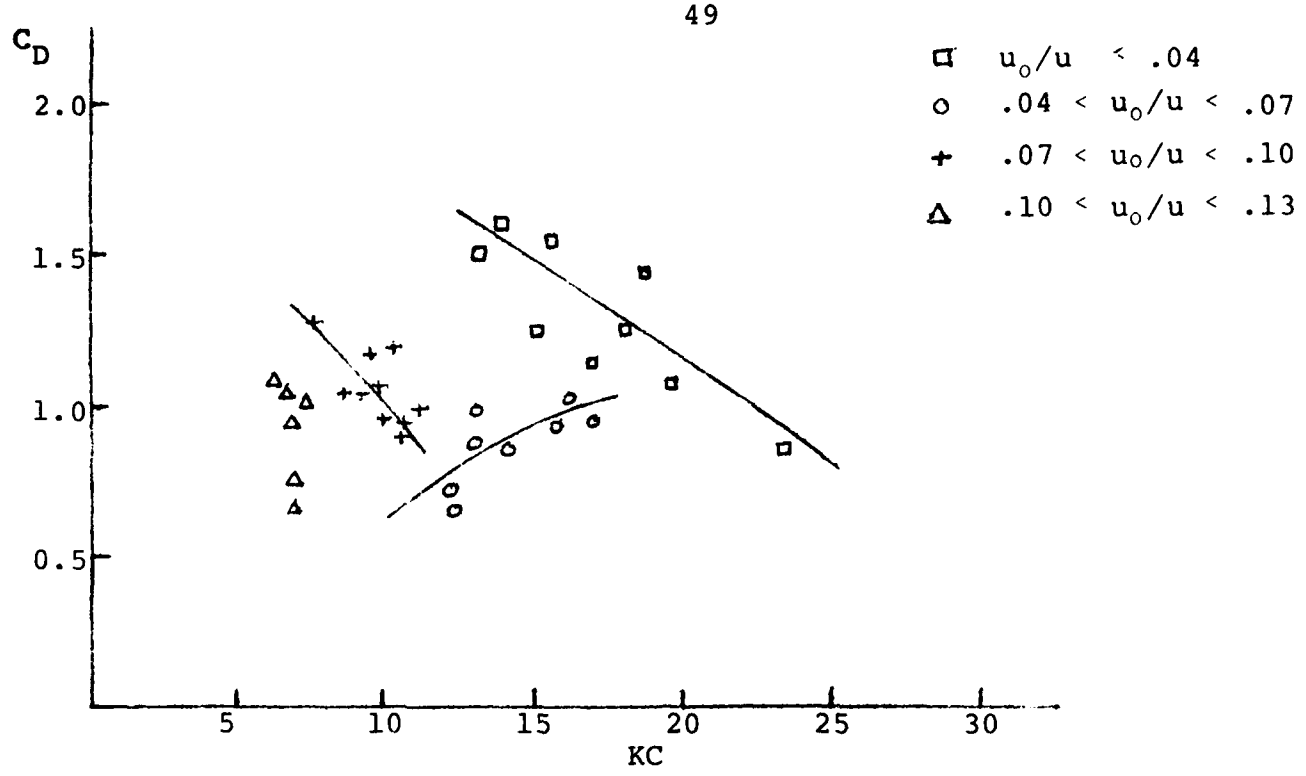

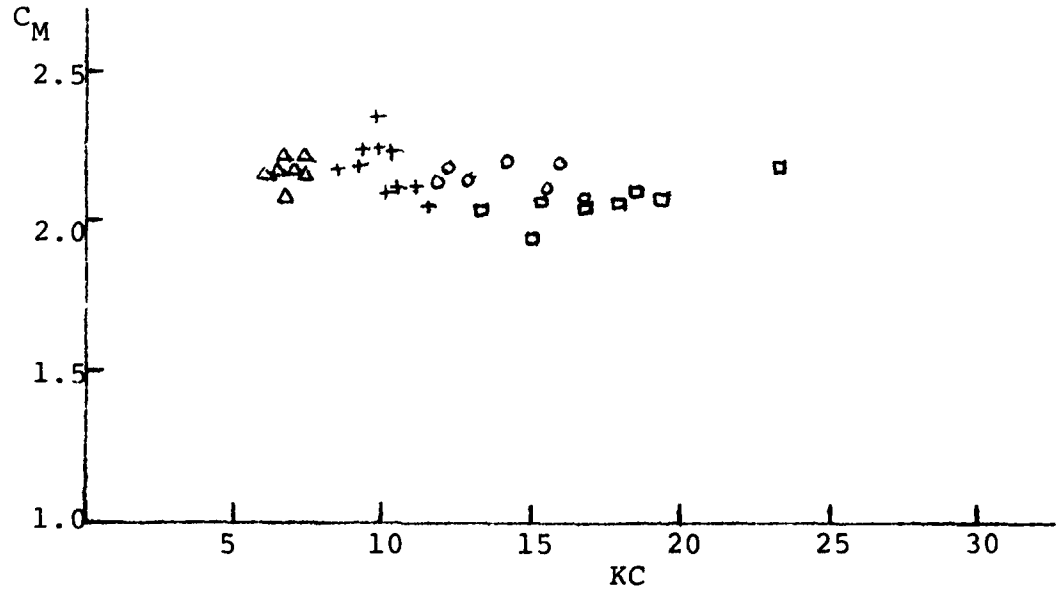

Fig. 12 C_D and C_M variation with KC, for different relative current values, C-waves and LS8A waves, NW (painted) element, $\beta \simeq 26{,}000$ (average).

The same type of graphical plots were made for the SS9 wave segment results, with the relative current velocity ratio u_o/u extending to values about 4 times as large as for the previous data from the C-wave and LS8A records. The β values for which the data were grouped were 14,000, 18,000 and 22,000, where these values were the midpoint average of values extending up to ±2,000 about these average reference values. The results of the system identification procedure, i.e. the values of C_D and C_M found from that type of analysis, are shown plotted as a function of KC for each β value range in Figures 13-15. The parametric dependency of the current velocity ratio is exhibited by means of different symbols, as shown in the legend for each figure.

A number of observations are made concerning this data, which corresponds to an unpainted sensor element (SW leg) that would be subject to marine growth bio-fouling and hence would have some degree of natural roughness. The total number of records analyzed for this case is much less than the data for the painted NW leg, and this is manifested in a reduced degree of overlap of data points (with different relative current ratio values) over a similar range of KC values. The magnitudes of C_D are generally larger for this data when compared with the values for the unpainted leg data, which is consistent with results of other analyses of the OTS data (e.g. see [6]) as well as the general result for increased C_D for rough cylinders in the same type of oscillatory flow where compared to a smooth cylinder.

There is also a large range of scatter in the C_D values, without any consistency that can be ascribed to the effect of a current. A possible cause of the scatter could be considered to be due to the effects of the transport operation on the measured velocities at the SE leg, but the results of [9] and other related studies that included such transport operations did not indicate any large influence on the coefficient values that would produce such a large scatter. A larger data set could possibly provide more points in the figures that could lead to an observable trend that could be related to the influence of the current. Only a liberal interpretation of the C_D values for the different relative current value, as shown in Figures 14 and 15, would allow a conclusion that the C_D values decreased with an increase in the relative current ratio value. Replotting the data in these figures (Fig. 13-15) in terms of the current parameter expressed by the quantity V_R, as was done in [5], also did not exhibit any definitive trend for different ranges of the parameter V_R.

There are a large number of force coefficient values concentrated in the KC range from 10-20, which is the generally devoted range indicating drag-inertia dominance. The significant scatter of results in the region may be due to some effect

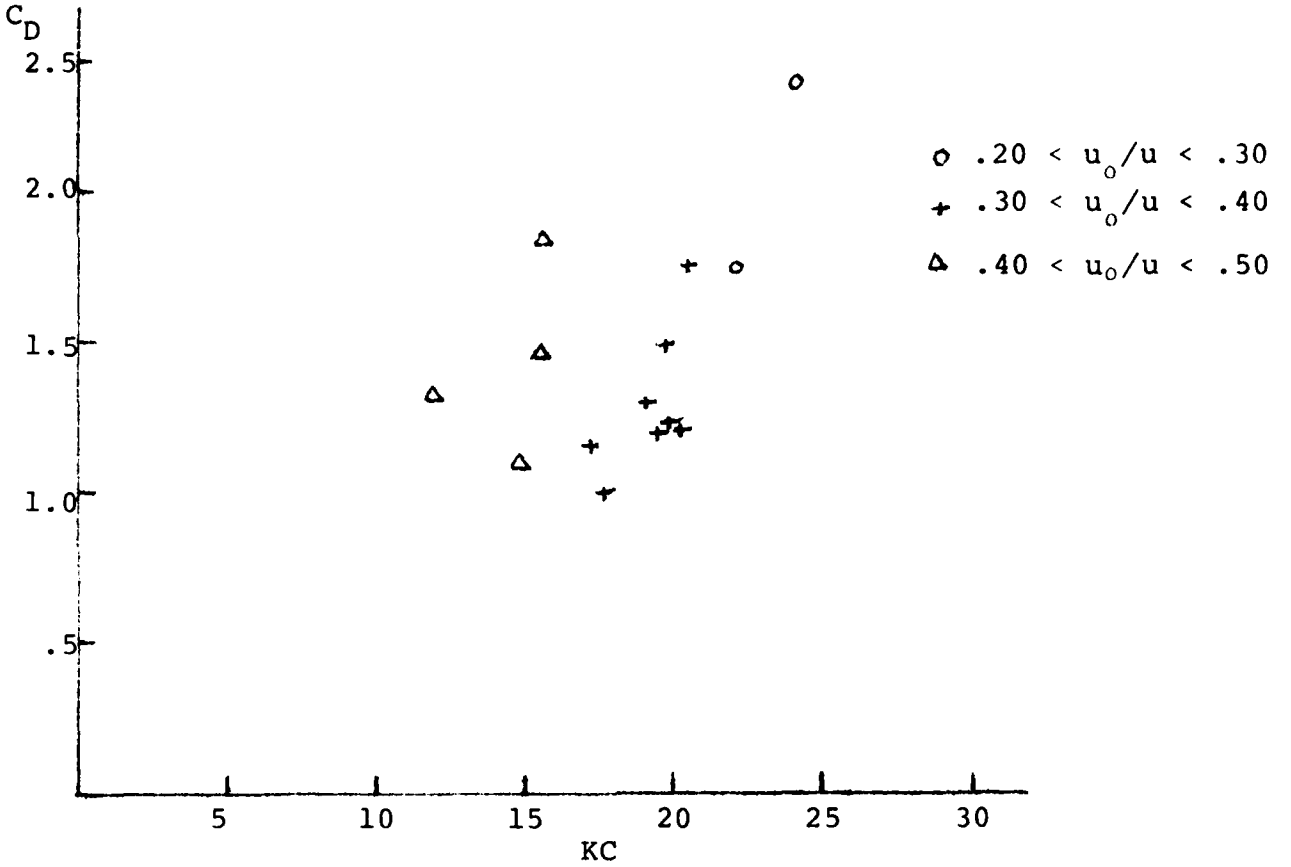

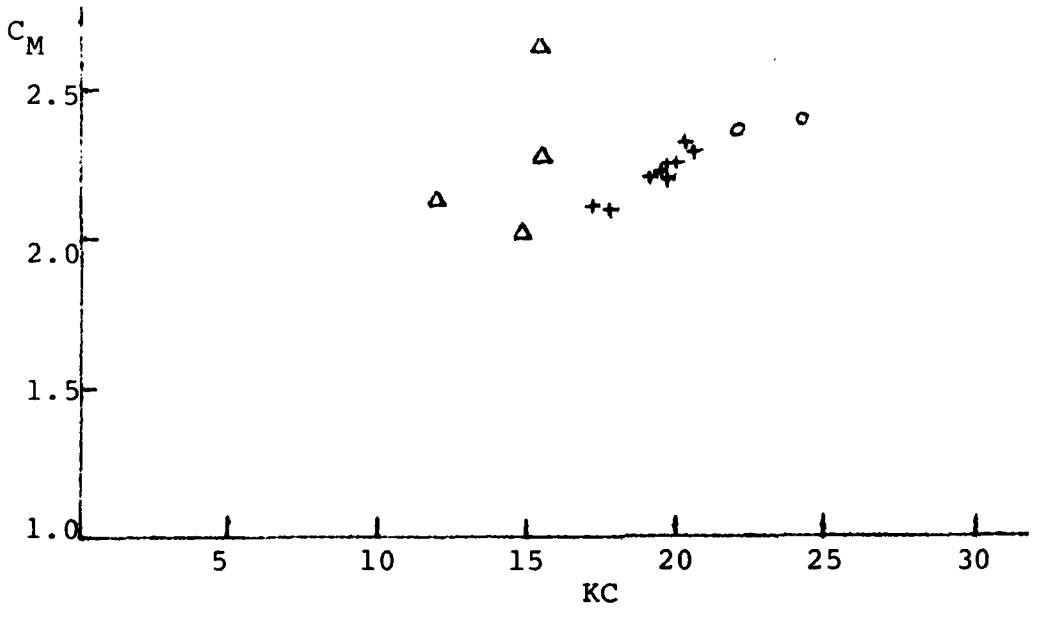

Fig. 13 C_D and C_M variation with KC, for different relative current values, SS9 waves, SW (unpainted) element, $\beta \simeq 14{,}000$ (average)

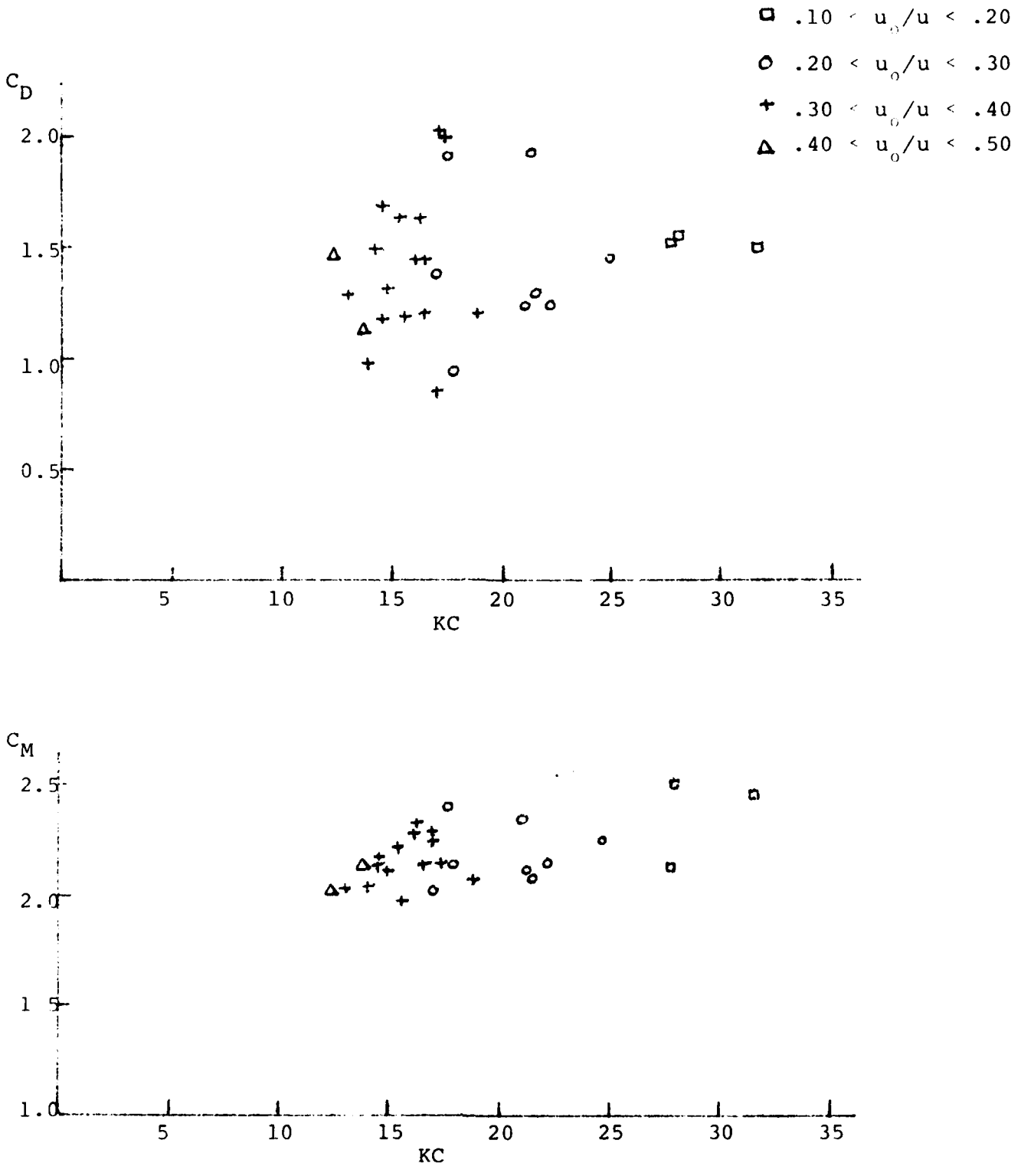

Fig. 14 C_D and C_M variation with KC, for different relative current values, SS9 waves, SW (unpainted) element, R~18,000 (average)

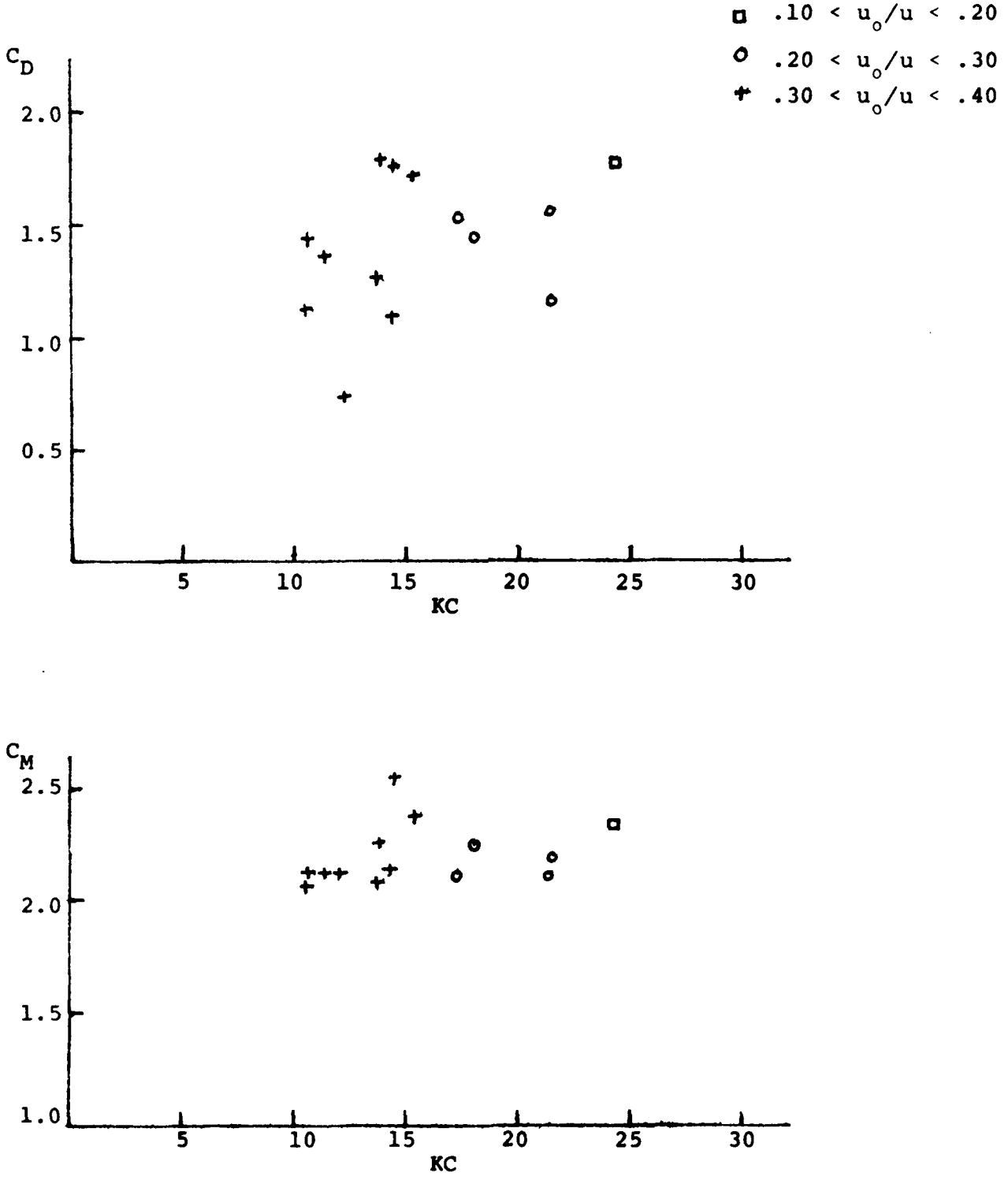

Fig. 15 C_D and C_M variation with KC, for different relative current values, SS9 waves, SW (unpainted) element, $\beta \approx 22{,}000$ (average)

of the current, or may be a manifestation of the general flow complexity in that range for realistic field measurements and related analyses. The same characteristic of scatter in the values of the inertia coefficient C_M occur as well as for C_D, with the C_M value extending up to somewhat larger values in this range than for the smooth painted cylinder results.

As described above, the coefficients determined from the system identification analysis for the present data set from the OTS investigation, did not provide a definitive trend that could illustrate the effect of current on the forces in waves. While some trend, which supports the concept of reduction in C_D with increase in the current magnitude, was present there was no dominant effect precisely illustrated even in the case with larger current values. One important reason for this was the lack of enough data points, for different relative current values, over a sufficient extent of KC values that would allow an overlap of data throughout the KC range. Such a set would allow simple visual illustration in the figures of differences due to different relative current ratio values.

During the time of this investigation a separate study was being carried out in a laboratory test facility by Sarpkaya [18] to study the effects of a combined wave and current flow on cylinder hydrodynamic forces. Since the various flow parameters are more easily controlled in such a laboratory test, using the special oscillatory water tunnel developed by Sarpkaya, coverage of the overall KC range for different relative current ratio values was readily achieved. The re- results in [18] showed the drag-inertia dominant region (KC range about 6-20), with the increasing current value leading to a reduction of C_D in that range. The effect of the current, which is ascribed to wake-biasing in [18], also increases C_M in that same range.

While the results of [18] demonstrate the above effects, and the conclusion that force coefficient values found for the case of no current cannot adequately predict the forces arising from a combined current and wave flow, the same type result was not directly indicated (with enough definitive supportive data) in the present investigation using real ocean field data and a system identification analysis that demonstrated good coefficient values fitting the measured data. Some aspects of agreement with the results of [18] were indicated, but others were not. In particular the inertia coefficient C_M does not show any significant dependence on KC or the current parameter, with its value always around 2.0 or somewhat larger (up to about 2.6) This characteristic is always indicated by results of system identification studies (e.g. [15]) applied to ocean data, with such a result differing from values found by any other analysis method.

The occurrence of a major influence of a current on force coefficients in the drag-inertia dominant region (KC range 6-20) also indicates the possible occurrence of scatter in data analysis results for force coefficients since the flow field complexity in that region generally exhibits scatter in coefficient values associated with that range when analyzing real ocean field data (e.g. see [6]). The effects of wave orbital velocities, the possible influence of different directions of the current and the in-line wave velocity, effects of spacial coherence in a real ocean flow field, etc. may be contributing effects that do not allow a definitive influence of current to be exhibited in the present force coefficient data.

The range of relative current ratios, V_R values, in the present data exceeds somewhat the maximum values in [18] (and also in [5]), but there is no significant trend of current effects shown in the present results. The influence of the various other factors discussed above may be over-riding or masking the direct current effect in the present data. Another possibility that could influence the present results, in contrast to that in [18], is that the Re values are much lower for the data in [18] (as evidenced by the β values there) than in the present ocean field data case.

Considering all of these features and the present results, the only basic utility of the force coefficient results from the present tests is the values of the coefficients themselves. These values, and their variations with pertinent dimensionless parameters as given in Table 1-3 and Figures 10-15, represent another contribution to a data base for wave force coefficients that have been determined from analysis of realistic ocean data. Such information can be used, toether with additional guidance from theory and related laboratory model test data, to provide suggested values of force coefficients for use in Morison equation applications for offshore structure design.

CONCLUDING REMARKS

The present analysis has demonstrated the utility of a previously applied technique of system identification to determine the values of the inertia and drag coefficients in the Morison equation representation of wave forces on an instrumented segment of an offshore structure; even when a current is part of the incident flow field. The procedure includes an on-line filtering action, as well as providing a measure of how well the estimated forces, velocities, etc. match the measured values throughout the entire measured time histories. The values of the force coefficients found by this method in the present study are found to be reasonably constant, and the Morison equation model suitability as a means of representing the wave forces in the presence of a current is generally exhibited by these results.

The force coefficient values found in this study do not exhibit any definitive variations with a current parameter, although there is some indication of a reduction of C_D as the relative current ratio increases. The result of actual data from the field measurements do not provide an adequate range coverage of all pertinent parameters such as KC and the relative current ratio that could indicate a definite trend in the data. The inertia coefficient C_M does not exhibit any significant variability with these parameters, with the C_M values generally being in the range of 2.0-2.6 for all of the conditions considered.

The data obtained from this study, which represents 222 sets of coefficients from an analysis of forces on both smooth (painted) and slightly rough (unpainted) elements of an offshore structure, can be used as part of a data base for establishing design ranges of such force coefficients. As such it provides an additional set of values, which have been demonstrated to have validity as a result of their matching of measured forces, for use in establishing such engineering tools that can be applied for offshore structure design.

REFERENCES

1. Morison, J.R., O'Brien, M.P., Johnson, J.W. and Scaaf, S.A.: "The Force Exerted by Surface Waves on Piles," Petroleum Trans., Vol. 189, TP 2846, 1950.

2. Sarpkaya, T.: "Morison's Equation and the Wave Forces on Offshore Structures," Naval Civil Eng. Lab. CR 82.008, Dec. 1981.

3. Sarpkaya, T. and Isaacson, M.: Mechanics of Wave Forces on Offshore Structures, Van Nostrand Reinhold, New York, 1981.

4. Kaplan, P. and Bentson, J.: "An Investigation of the Utility of the Morison Equation for Relative Motion Applications," Proc. 3rd OMAE Symposium, ASME, New Orleans, La., Feb. 1984.

5. Sarpkaya, T. and Cakal, I.: "A Comprehensive Sensitivity Analysis of the OTS Data," Proc. of OTC, OTC 4616, 1983.

6. Heideman, J. C., Olsen, O. A. and Johansson, P. I." "Local Wave Force Coefficients," Civil Engineering in the Oceans IV, ASCE, Vol. 1, Sept. 1979.

7. Haring, R.E. and Spencer, L.P.: "The Ocean Test Strucutre Data Base," Civil Engineering in the Oceans IV, ASCE, Vol. 1, Sept. 1979.

8. Richman, G. and Bendat, J.S.: "Time Series Analysis of Ocean Test Structure Data, an Interim Report," Vols. 1 & 2, MRI Rpt. TML01, 13 Jan. 1978.

9. Kaplan, P., Jiang, C. W. and Dello Stritto, F.J.: "Force Coefficient Evaluation for Offshore Structure Inclined Members," Proc. BOSS '82, M.I.T., Cambridge, Mass., Aug. 1982.

10. Kaplan, P., Sargent, T.P. and Goodman, T.R.: "The Application of System Identification to Dynamics of Naval Craft," Proc. Ninth Symp. on Naval Hydrodynamics, Office of Naval Research, 1972.

11. Detchmendy, D.M. and Sridhar, R.: "Sequential Estimation of States and Parameters in Noisy Nonlinear Dynamic Systems," J. of Basic Engineering, ASME, June 1966.

12. Bellman, R.E., Kagiwada, H.H., Kalaba, R.E. and Sridhar, R.: "Invariant Imbedding and Nonlinear Filtering Theory," Rand Corp., Memorandum RM-4374-PR, Dec. 1964.

13. Lee, E.S.: Quasilinearization and Invariant Imbedding, Vol. 41, Mathematics in Science and Engineering, Academic Press, 1968.

14. Kalman, R.E. and Bucy, R.S.: "New Results in Linear Filtering and Prediction Theory," J. Basic Engineering, Vol. 83, No. 95, 1961.

15. Kaplan, P., Jiang, C. W. and Dello Stritto, F.J.: "Determination of Offshore Structure Morison Equation Force Coefficients via System Identification Techniques," Proc. of Int. Symposium on Hydrodynamics in Ocean Engineering, Trondheim, Norway, 1981.

16. Sage, A.P. and Melsa, J.L.: System Identification, Vol. 80 Mathematics in Science and Engineering, Academic Press, 1971.

17. Verly, R.L. and Moe, G.: "The Forces on a Cylinder Oscillating in a Current," River and Harbor Lab., The Norwegian Inst. of Tech., Rpt. No. STF60 A79061, 1979.

18. Sarpkaya, T., Bakmis, C. and Storm, M.A.: "Hydrodynamic Forces From Combined Wave and Current Flow on Smooth and Rough Circular Cylinders at High Reynolds Numbers," Proc. of OTC, OTC 4830, 1984.

END

FILMED

3-85

DTIC